

ADA100 298

ADA100298
TECHNICAL
LIBRARY



AD

TECHNICAL REPORT ARBRL-TR-02315

EXPERIMENTAL STUDIES OF IGNITION PHENOMENA
IN ONE-DIMENSIONAL PROPELLING CHARGES

Thomas C. Minor
Albert W. Horst

April 1981



US ARMY ARMAMENT RESEARCH AND DEVELOPMENT COMMAND
BALLISTIC RESEARCH LABORATORY
ABERDEEN PROVING GROUND, MARYLAND

Approved for public release; distribution unlimited.

Destroy this report when it is no longer needed.
Do not return it to the originator.

Secondary distribution of this report by originating
or sponsoring activity is prohibited.

Additional copies of this report may be obtained
from the National Technical Information Service,
U.S. Department of Commerce, Springfield, Virginia
22161.

The findings in this report are not to be construed as
an official Department of the Army position, unless
so designated by other authorized documents.

*The use of trade names or manufacturers' names in this report
does not constitute endorsement of any commercial product.*

UNCLASSIFIED

SECURITY CLASSIFICATION OF THIS PAGE (When Data Entered)

REPORT DOCUMENTATION PAGE		READ INSTRUCTIONS BEFORE COMPLETING FORM
1. REPORT NUMBER TECHNICAL REPORT ARBRL-TR-02315	2. GOVT ACCESSION NO.	3. RECIPIENT'S CATALOG NUMBER
4. TITLE (and Subtitle) Experimental Studies of Ignition Phenomena in One-Dimensional Propelling Charges		5. TYPE OF REPORT & PERIOD COVERED Technical Report Oct 78 - Sep 79
		6. PERFORMING ORG. REPORT NUMBER
7. AUTHOR(s) Thomas C. Minor and Albert W. Horst		8. CONTRACT OR GRANT NUMBER(s)
9. PERFORMING ORGANIZATION NAME AND ADDRESS US Army Ballistic Research Laboratory ATTN: DRDAR-BLI Aberdeen Proving Ground, MD 21005		10. PROGRAM ELEMENT, PROJECT, TASK AREA & WORK UNIT NUMBERS 1L162618AH80
11. CONTROLLING OFFICE NAME AND ADDRESS US Army Armament Research & Development Command US Army Ballistic Research Laboratory ATTN: DRDAR-BL Aberdeen Proving Ground, MD 21005		12. REPORT DATE APRIL 1981
		13. NUMBER OF PAGES 58
14. MONITORING AGENCY NAME & ADDRESS (if different from Controlling Office)		15. SECURITY CLASS. (of this report) Unclassified
		15a. DECLASSIFICATION/DOWNGRADING SCHEDULE
16. DISTRIBUTION STATEMENT (of this Report) Approved for public release; distribution unlimited.		
17. DISTRIBUTION STATEMENT (of the abstract entered in Block 20, if different from Report)		
18. SUPPLEMENTARY NOTES		
19. KEY WORDS (Continue on reverse side if necessary and identify by block number) Interior Ballistics Model Validation Flamespreading Pressure Waves Computer Codes		
20. ABSTRACT (Continue on reverse side if necessary and identify by block number) nlg During the past decade, several unsteady, two-phase flow interior ballistic models have been developed which include treatment of ignition and flamespread through the propellant bed. While all such models were originally formulated under the simplifying assumption of one-dimensional flow, efforts are now under-way to provide multi-dimensional representations, as well as to improve the descriptions of constitutive physical processes. One important step, however, along the road to a phenomenologically complete model should be a critical		

UNCLASSIFIED

SECURITY CLASSIFICATION OF THIS PAGE(When Data Entered)

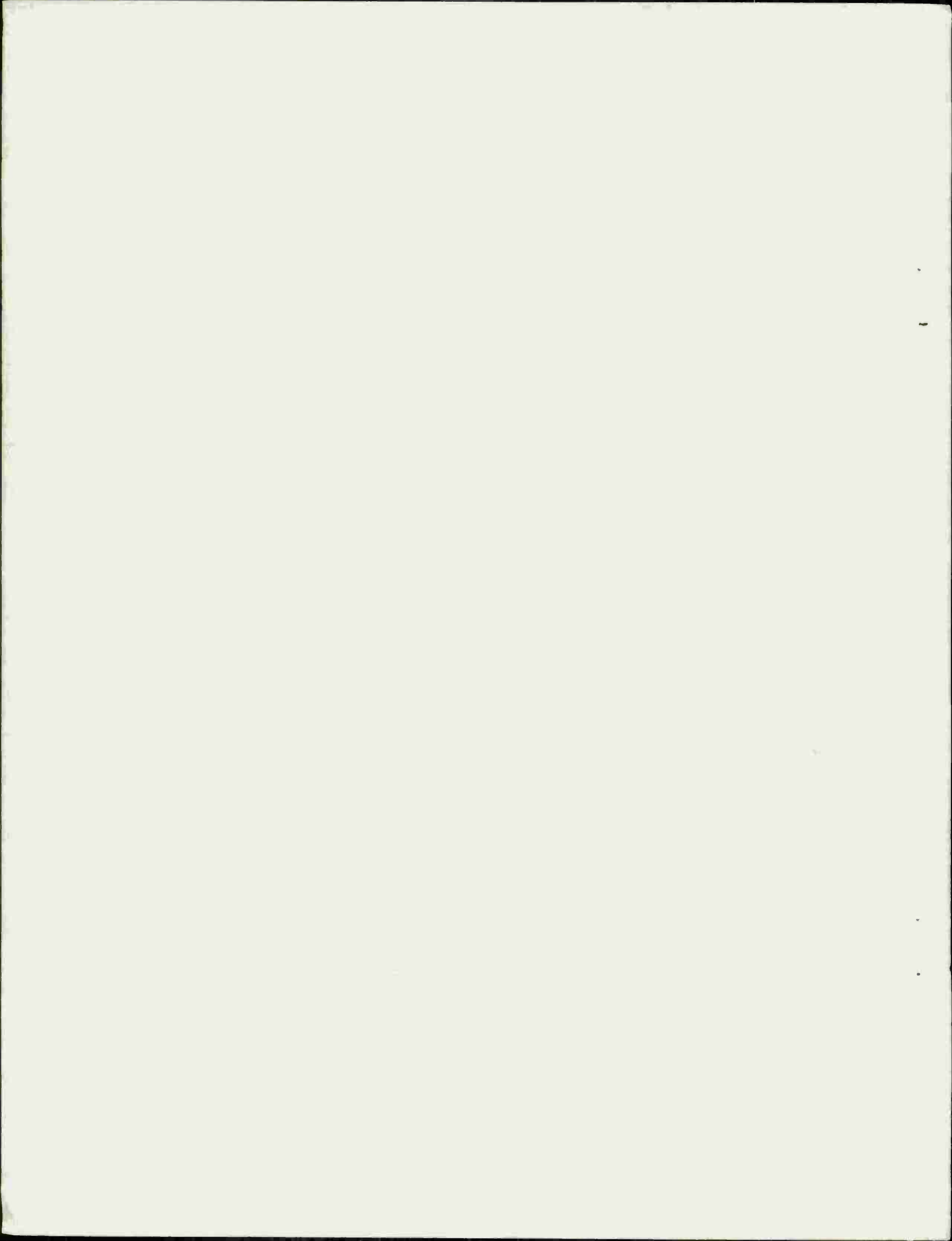
assessment of available one-dimensional codes by means of comparison to "one-dimensional" experiments. To that end, we describe herein a series of four, well-instrumented, "one-dimensional," test firings conducted in the Navy 5-inch fiberglass breech gun. Two rounds were fired using Navy NOSOL 318 propellant, a solventless-processed gun propellant offering excellent control over grain dimensions and physical and chemical homogeneity. The other two rounds were fired with M30A1 triple-base gun propellant, employed in the Army 155-mm, M203, Propelling Charge. Data recorded during these tests included flame propagation, breech and sidewall gas pressure profiles, and sidewall case strains. Comparisons of experimental results with sample theoretical simulations of these events using the NOVA two-phase flow interior ballistics code are presented both to suggest possible areas of future concern to model developers and to assess the adequacy of current experimental techniques.

UNCLASSIFIED

SECURITY CLASSIFICATION OF THIS PAGE(When Data Entered)

TABLE OF CONTENTS

	Page
LIST OF ILLUSTRATIONS	5
I. INTRODUCTION.	7
II. TECHNICAL DISCUSSION.	7
A. Phenomenology of the Gun Interior Ballistic Cycle . .	7
B. Recent Advances in Interior Ballistic Modeling. . . .	11
C. The Requirement for Experimentation.	13
III. EXPERIMENTAL.	14
A. One-Dimensional, NOSOL 318 Tests.	16
B. One-Dimensional, M30A1 Tests.	28
IV. CONCLUSIONS	33
ACKNOWLEDGMENTS	36
REFERENCES.	37
APPENDIX A.	41
APPENDIX B.	47
DISTRIBUTION LIST	53



LIST OF ILLUSTRATIONS

Figure	Page
1. Schematic of Gun Propelling Charge	9
2. Pressure-Time and Pressure-Difference Profiles - Ideal.	9
3. Pressure-Time and Pressure-Difference Profiles, 175-mm Breechblow.	10
4. 5-Inch Fiberglass Breech Gun, Naval Surface Weapons Center, Dahlgren, Virginia	15
5. Charge Schematic, 5-Inch, One-Dimensional Tests.	16
6. 5-Inch, One-Dimensional Igniter.	17
7. Experimental Piezoelectric Pressures, NOSOL 318 Propellant	19
8. Experimental Piezoelectric Pressure Profiles, NOSOL 318 Propellant	19
9. Experimental Strain Pressures, NOSOL 318 Propellant. . . .	20
10. Experimental Strain Pressure Profiles, NOSOL 318 Propellant	20
11. Comparison of Experimental Piezoelectric and Strain Pressures, NOSOL 318 Propellant.	21
12. Simplified Igniter Output Profiles (Input to NOVA Code). .	23
13. One-Dimensional Igniter Static Firing Results.	24
14. Comparison of Experimental and Calculated Pressures, NOSOL 318 Propellant	25
15. Comparison of Predicted and Experimental Pressure- Difference Profiles ($P_1 - P_5$) for NOSOL 318.	26
16. Experimental and Calculated Flame and Pressure Fronts for NOSOL 318 Propellant	27
17. Flamespread, M30A1 Propellant.	29

LIST OF ILLUSTRATIONS (Continued)

Figure	Page
18. Experimental Piezoelectric Pressures, M30A1 Propellant. . .	30
19. Experimental Piezoelectric Pressure Profiles, M30A1 Propellant.	30
20. Experimental Strain Pressures, M30A1 Propellant	31
21. Experimental Strain Pressure Profiles, M30A1 Propellant . .	31
22. Comparison of Experimental Piezoelectric and Strain Pressures, M30A1 Propellant	32
23. Comparison of Experimental and Calculated Pressures, M30A1 Propellant.	34
24. Experimental and Calculated Flame and Pressure Fronts for M30A1 Propellant.	35

I. INTRODUCTION

Major advances in our understanding of the detailed phenomenology of the gun interior ballistics cycle have occurred over recent years. Much of this progress has resulted from theoretical and experimental efforts undertaken in response to a recognition of the interior ballistics cycle as an unsteady, two-phase flow problem, in which events occurring during the ignition/flamespread portion may have dramatic impact on the overall process. Thus a whole new field of interior ballistics modeling, including the processes of ignition and flamespread, was founded and with it the need for experimental data both for model validation and guidance in future efforts.

This report describes a series of experiments designed to provide such data, as well as a comparison of experiment to theory, the theoretical values being provided by a set of sample calculations performed using an available one-dimensional, two-phase flow, interior ballistics code. While a critical assessment of the code itself is outside the scope of this report, apparent strengths and weaknesses of the simulations are noted, and areas of possible future interest to both model developers and experimental investigators are suggested.

II. TECHNICAL DISCUSSION

A. Phenomenology of the Gun Interior Ballistic Cycle

While the overall gun interior ballistic cycle involves an extremely complex interplay of chemical and physical processes, classical pictures of it have often invoked major simplifying assumptions to facilitate model formulation. A typical lumped-parameter model¹ is based on instantaneous, or at least simultaneous, uniform ignition of the entire propellant bed, followed by a spacewise-averaged thermodynamic treatment of what is viewed to be a well-stirred mixture of propellant gas and particles. A simplified description of the pressure gradient is superimposed on this solution only for purposes of calculating maximum breech pressure and the force profile on the projectile base, integration of which allows calculation of projectile velocity and travel.

In actual practice, this artificially imposed decoupling of ignition and combustion events is far from phenomenologically correct, and flow dynamics accompanying flamespread may exhibit a significant impact on the remainder of the interior ballistic cycle. This influence

¹P. G. Baer and J. M. Frankle, "The Simulation of Interior Ballistic Performance of Guns by Digital Computer Program," Report 1183, Ballistic Research Laboratories, Aberdeen Proving Ground, MD, December 1961. (AD #299980)

is best demonstrated by specifically addressing the functioning of an idealized (though certainly not ideal) granular propellant charge, as shown in Figure 1. Typically an igniter system is electrically or mechanically initiated, leading to the venting of high-temperature, combustion products into a bed of granular propellant. The intensity and geometrical distribution of this output varies significantly with the system. The surfaces of nearby propellant grains are heated to a sufficient temperature to initiate combustion. Hot propellant gases then join those from the igniter to penetrate the rest of the bed, convectively heating the propellant and resulting in flamespread. During this phase, resistance to gas flow offered by the packed bed may result in large pressure gradients capable of leading to substantial propellant motion. In particular, localized ignition at the base of the propellant bed with ullage, or free space, present at the other end (between the charge and the projectile base) can lead to large forward velocities of both gas and solid phases. Stagnation at the projectile base is then accompanied by a substantial level of local pressurization, bed compaction, and perhaps even grain fracture². In the limit, the ideal pressure-time curves shown in Figure 2 give way to the very real profiles shown in Figure 3, which depicts an over-pressurization leading to a breechblow in a 175-mm gun. These figures also illustrate a procedure now employed by many ballisticians, wherein pressure-time data recorded at the projectile end of the chamber are subtracted from corresponding data taken at the breech end to yield the "pressure-difference profile." This curve provides a convenient, graphic portrayal of the evolution of longitudinal pressure waves in gun chambers.

A rigorous understanding of those processes involved in the formation of pressure waves and their impact on the rest of the interior ballistic cycle is needed if one is to be able to make meaningful predictions about the performance and safety of new charge designs. Of at least equal importance is the need to provide a useful diagnostic capability with respect to anomalous behavior exhibited by existing charges. Accurate quantitative statements on any of these matters require the formulation of an adequate interior ballistic model which includes treatment of all important physical and chemical processes involved in flamespread, the formation of pressure waves, and their coupling with maximum chamber pressures. For the experimentalist, this means that he is called upon first to assist in identifying those processes which must be considered in the physical scope of the model, and second to provide data for validation of the adequacy of the physical representation and numerical procedures.

²A. W. Horst, I. W. May, and E. V. Clarke, "The Missing Link Between Pressure Waves and Breechblows," 14th JANNAF Combustion Meeting, CPIA Publication 292, Vol. II, pp. 277-292, December 1977.

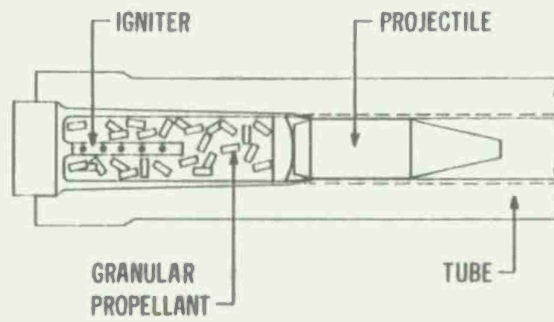


Figure 1. Schematic of Gun Propelling Charge

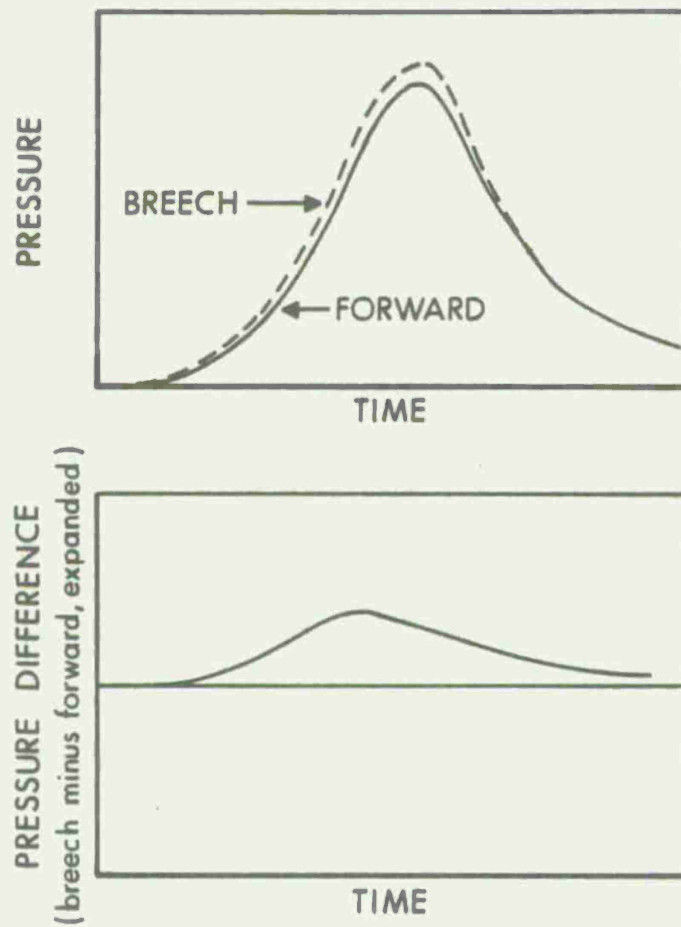


Figure 2. Pressure-Time and Pressure-Difference Profiles - Ideal

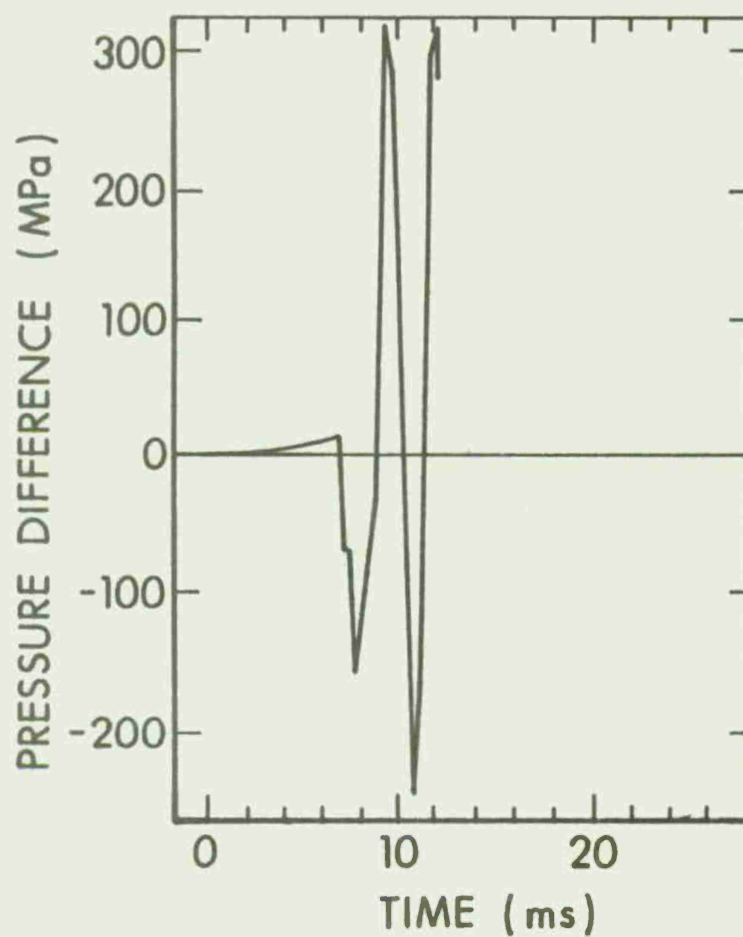
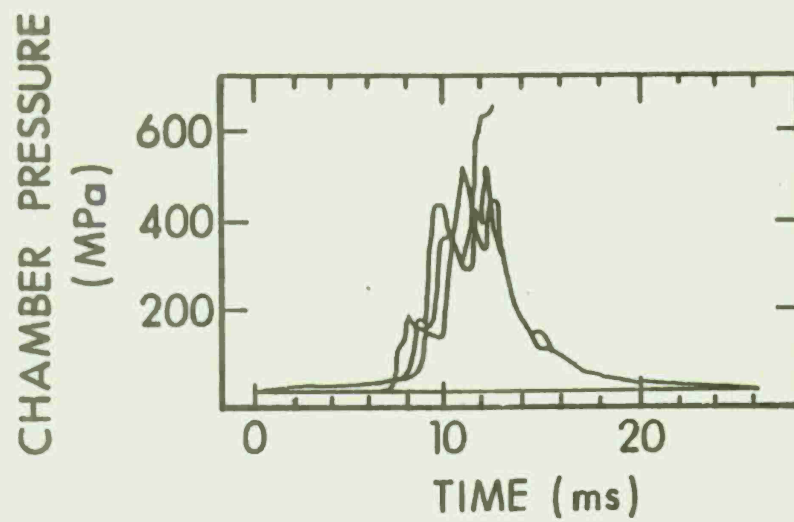


Figure 3. Pressure-Time and Pressure-Difference Profiles, 175-mm Breechblow

B. Recent Advances in Interior Ballistic Modeling

This past decade has seen considerable activity in the field of modeling unsteady, multiphase flows. A small sample of the nature and complexity of such work was recently revealed at an Army Research Office Workshop on Multiphase Flows³. One subset of this field has been that of flamespread and combustion in a mobile, granular propellant bed. These studies are of particular interest in terms of their relevance to ignition transients, pressure waves, and even breechblows in Army artillery and tank guns. The works of several US flamespread modelers were reviewed in a Joint-Army-Navy-NASA-Air Force (JANNAF) Workshop⁴ several years earlier. Since that time, modeling of flamespread and pressure-wave phenomena in the gun environment has received further attention principally by Fisher^{5,6}, Gough⁷⁻⁹, and Kuo¹⁰. Several

³J. Chandra and C. Zoltani, "Proceedings of ARO Workshop on Multiphase Flows," US Army Research Office and the Ballistic Research Laboratory, Aberdeen Proving Ground, MD, February 1978.

⁴K. K. Kuo, "A Summary of the JANNAF Workshop on Theoretical Modeling and Experimental Measurements of the Combustion and Fluid Flow Processes in Gun Propellant Charges," 13th JANNAF Combustion Meeting, CPIA Publication 281, Vol. I, pp. 213-233, December 1976.

⁵E. B. Fisher, "Quality Control of Continuously Produced Gun Propellant," Calspan Report No. SA-5913-X-1, Calspan Corporation, Buffalo, NY, August 1977.

⁶E. B. Fisher, "Investigation of Breechblow Phenomenology," Contract Report ARBRL-CR-00412, Ballistic Research Laboratory, USA ARRADCOM, Aberdeen Proving Ground, MD, January 1980. (AD #B046080L)

⁷P. S. Gough and F. J. Zwarts, "Some Fundamental Aspects of the Digital Simulation of Convective Burning in Porous Beds," AIAA/SAE 13th Propulsion Conference, AIAA Paper No. 77-855, July 1977.

⁸P. S. Gough, "Theoretical Study of Two-Phase Flow Associated with Granular Bag Charges," Contract Report ARBRL-CR-00381, Ballistic Research Laboratory, USA ARRADCOM, Aberdeen Proving Ground, MD, September 1978. (AD #A062144)

⁹P. S. Gough, "Two-Dimensional Convective Flamespreading in Packed Beds of Granular Propellant," Contract Report ARBRL-CR-00404, Ballistic Research Laboratory, USA ARRADCOM, Aberdeen Proving Ground, MD, July 1979. (AD #A075326)

¹⁰K. K. Kuo and J. H. Koo, "Transient Combustion in Granular Propellant Propellant Beds. Part 1: Theoretical Modeling and Numerical Solution of Transient Combustion Processes in Mobile Granular Propellant Beds," Contract Report No. 346, Ballistic Research Laboratory, USA ARRADCOM, Aberdeen Proving Ground, MD, August 1977. (AD #A044998)

other efforts^{11,12} recently sponsored by the US Army are currently addressing post-flamespread phenomena and, hence, are not relevant to the description of ignition/combustion-driven pressure waves and attendant problems.

Calculations included in this study were performed using the NOVA Code^{7,13-16} developed by Paul Gough Associates, under contract to the Naval Ordnance Station, Indian Head, MD. NOVA consists of a two-phase flow treatment of the gun interior ballistics cycle formulated under the assumption of quasi-one-dimensional flow. The balance equations describe the evolution of averages of flow properties accompanying changes in mass, momentum and energy and arising out of interactions associated with combustion, interphase drag and heat transfer. Constitutive laws include a covolume equation of state for the gas and an incompressible solid phase. Compaction of an aggregate of grains, however, is allowed, with granular stresses in excess to ambient gas pressure being taken to be in accord with steady state measurements. Interphase drag is represented by reference to the empirical, steady state correlations of Ergun¹⁷ and Andersson¹⁸ for fixed and fluidized beds respectively.

¹¹H. J. Gibeling, R. C. Buggeln and H. McDonald, "Development of a Two-Dimensional Implicit Interior Ballistics Code," Contract Report ARBRL-CR-00411, Ballistic Research Laboratory, USA ARRADCOM, Aberdeen Proving Ground, MD, January 1980. (AD #A084092)

¹²A.C. Buckingham, "Modeling Additive and Hostile Particulate Influences in Gun Combustion Turbulent Erosion," 16th JANNAF Combustion Meeting, CPIA Publication 308, Vol. I, pp. 673-690, December 1979.

¹³P. S. Gough and F. J. Zwarts, "Theoretical Model for Ignition of Gun Propellant," SRC-R-67, Space Research Corporation, North Troy, VT, December 1972.

¹⁴P. S. Gough, "Fundamental Investigation of the Interior Ballistics of Guns: Final Report," IHCR 74-1, Naval Ordnance Station, Indian Head, MD, August 1974.

¹⁵P. S. Gough, "Computer Modeling of Interior Ballistics," IHCR 75-3, Naval Ordnance Station, Indian Head, MD, October 1975.

¹⁶P. S. Gough, "Numerical Analysis of a Two-Phase Flow with Explicit Internal Boundaries," IHCR 77-5, Naval Ordnance Station, Indian Head, MD, April 1977.

¹⁷S. Ergun, "Fluid Flow Through Packed Columns," Chem. Eng. Progr., Vol. 48, pp. 89-95, 1952.

¹⁸K. E. B. Andersson, "Pressure Drop in Ideal Fluidization," Chem. Eng. Sci., Vol. 15, pp. 276-297, 1961.

Interphase heat transfer is described similarly according to Denton¹⁹ or Gelperin-Einstein²⁰. Functioning of the igniter is included by specifying a predetermined mass injection rate as a function of position and time. Flamespreading then follows from axial convection, with grain surface temperature being deduced from the heat transfer correlation and the unsteady heat conduction equation, and ignition based on a surface temperature criterion. In addition, propelling charge internal boundaries defined by discontinuity in porosity are treated explicitly, and the forward external boundary reflects the inertial and compactibility characteristics of any inert, packaging elements present between the propellant bed and the base of the projectile. Solutions are obtained using an explicit finite difference scheme based on the method of MacCormack²¹ for points in the interior and the method of characteristics at internal and external boundaries.

C. The Requirement for Experimentation

As noted earlier, considerable advancement has taken place over recent years in the field of two-phase flow, interior ballistic modeling. The qualitative features of longitudinal pressure waves in guns are well described in many instances by such models. Nevertheless, substantive, further advancement is necessary to extend their scopes of applicability to many current problems of interest (e.g., particularly those associated with bagged-charge phenomenology) and to provide truly quantitative statements concerning these problems.

Multi-dimensional flamespread and interior ballistic models are in various stages of development, but it is hardly likely that all shortcomings of existing models will disappear along with the elimination of the one-dimensional approximation. Indeed, critical examination of the applicability of "1-D" models to nearly one-dimensional charge configurations must be one step along the path to formulation of a phenomenologically complete model. Toward that end, we describe a set of experiments based on essentially a one-dimensional charge designed to provide data required for direct assessment of existing models. The experimental results obtained are compared to theoretical predictions of the NOVA interior ballistics code. We stress at the outset that no significant attempt was made to reconcile differences between experimental and theoretical results through manipulation of the input data. Rather, an

¹⁹W. H. Denton, "General Discussion on Heat Transfer," Inst. Mech. Eng. and Am. Soc. Mech. Eng., London, 1951.

²⁰N. I. Gelperin and V. G. Einstein, "Heat Transfer in Fluidized Beds," Fluidization, edited by J. F. Davidson and D. Harrison, Academic Press, 1971.

²¹R. W. MacCormack, "The Effects of Viscosity in Hypervelocity Impact Cratering," AIAA Paper No. 69-354, AIAA Aerospace Science Meeting, 1969.

input data base was assembled which was felt to be a reasonable compilation of currently available, independently determined values. The objectives of the comparison presented here are simply to identify apparent strengths and weaknesses as exemplified in the simulations provided and to assess the adequacy of current experimental techniques for model validation exercises.

III. EXPERIMENTAL

Firing tests were conducted for the Ballistic Research Laboratory at the Naval Surface Weapons Center, Dahlgren, Virginia, using Navy NOSOL 318 and Army M30A1 propellants. NOSOL 318 was chosen for testing because it is a solventless-processed gun propellant offering excellent dimensional stability and chemical and physical homogeneity as well as well-characterized burning rates. M30A1 was selected because it is the propellant used in the Zone 8, 155-mm, M203, Propelling Charge, and because no flamespread data previously existed for this formulation.

A photograph of the test fixture is shown in Figure 4. Central to the experiment is the Navy fiberglass breech gun²²⁻²⁴ with the disposable chamber made to simulate that of the 5-inch, 54-caliber gun. Chamber pressures were measured at the base of the case (P1) and at four sidewall locations (P2 through P5, running from the base to mouth of the case). In addition, axial case strains (S2 through S5) were recorded at approximately the locations of the sidewall pressure ports. Flamespread data were recorded on each shot using two Hycam high-speed cameras at framing rates of 5,000 and 10,000 frames per second. A common time base was provided between the analog and flamespread records through a timing signal recorded on the analog tape and the timing tracks of the film. Finally, an attempt was made at measuring movement of the propellant using dual flash X-rays to monitor the location of particular grains seeded with small brass rods.

²²J. L. East, "Experimental Techniques for Investigating the Start-Up Ignition/Combustion Transients in Full-Scale Charge Assemblies," 11th JANNAF Combustion Meeting, CPIA Publication 261, Vol. I, pp. 119-139, December 1974.

²³J. L. East and D. R. McClure, "Experimental Studies of Ignition and Combustion in Naval Guns," 12th JANNAF Combustion Meeting, CPIA Publication 273, Vol. I, pp. 221-257, December 1975.

²⁴W. R. Burrell and J. L. East, "Effects of Production Packing Depth and Ignition Techniques on Propelling Charge Reaction and Projectile Response," NSWC/DL TR-3705, Naval Surface Weapons Center, Dahlgren, VA, April 1978.

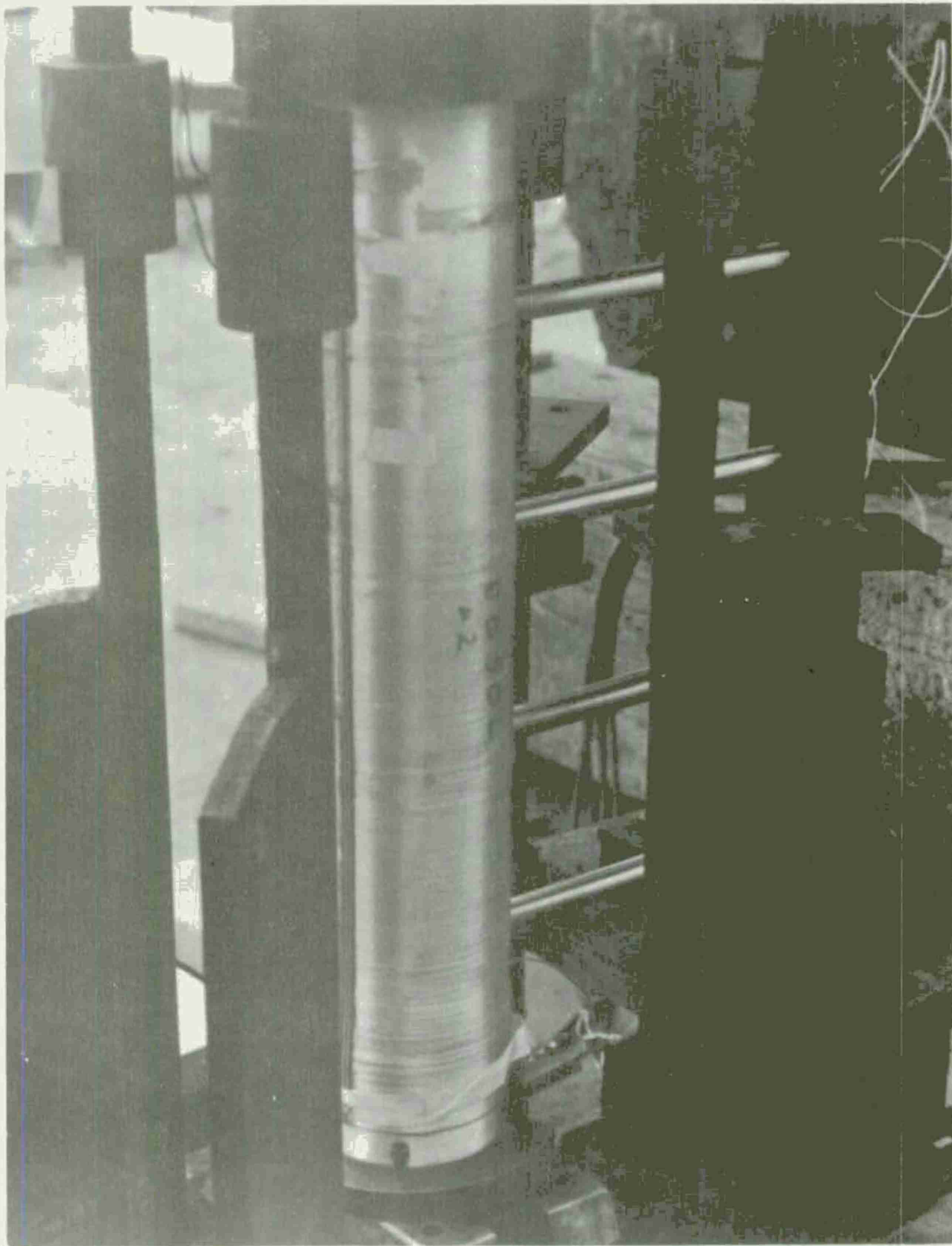


Figure 4. 5-Inch Fiberglass Breech Gun, Naval Surface Weapons Center, Dahlgren, Virginia

A schematic of the one-dimensional charges fired is shown in Figure 5. The propellant was loaded full-diameter with a packing depth of approximately 7.6 cm. The propellant was ignited with a specially built basepad, shown in Figure 6 from the rear (upper left), from the front (upper right), and partially disassembled, from the front (bottom of figure). This basepad was designed to provide a planar output, and preserve the one-dimensionality of the experiment. The pad consisted of 85 g of Class I black powder, ignited by a spiral wrap of mild detonating cord, supported on a wire grid. The cord was electrically initiated. There were no wads or closure plugs at the forward end of the charge, and with the exception of the first NOSOL 318 shot, the projectile was constrained from movement.

A. One-Dimensional, NOSOL 318 Tests

The NOSOL 318 propellant grains used for these shots had seven perforations, a length of 23.1 mm, an outer diameter of 11.6 mm, and a perforation diameter of 0.84 mm. The propellant charge mass was 9.27 kg. The initial axial ullage on the first shot was 34 mm, and the projectile traveled 19 mm during the event. The luminous output of the burning propellant was so low that flamespreading rates could not be determined. The other NOSOL 318 firing reproduced the first, so only one is reported in detail here.

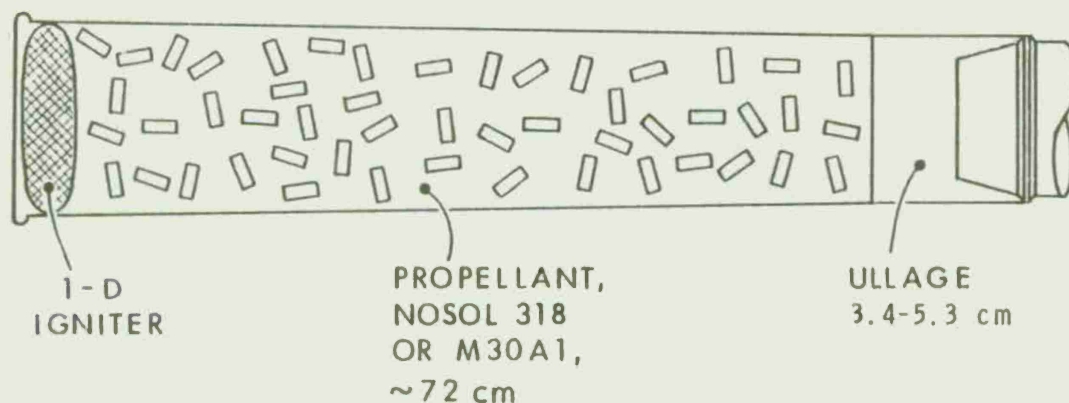


Figure 5. Charge Schematic, 5-Inch, One-Dimensional Tests

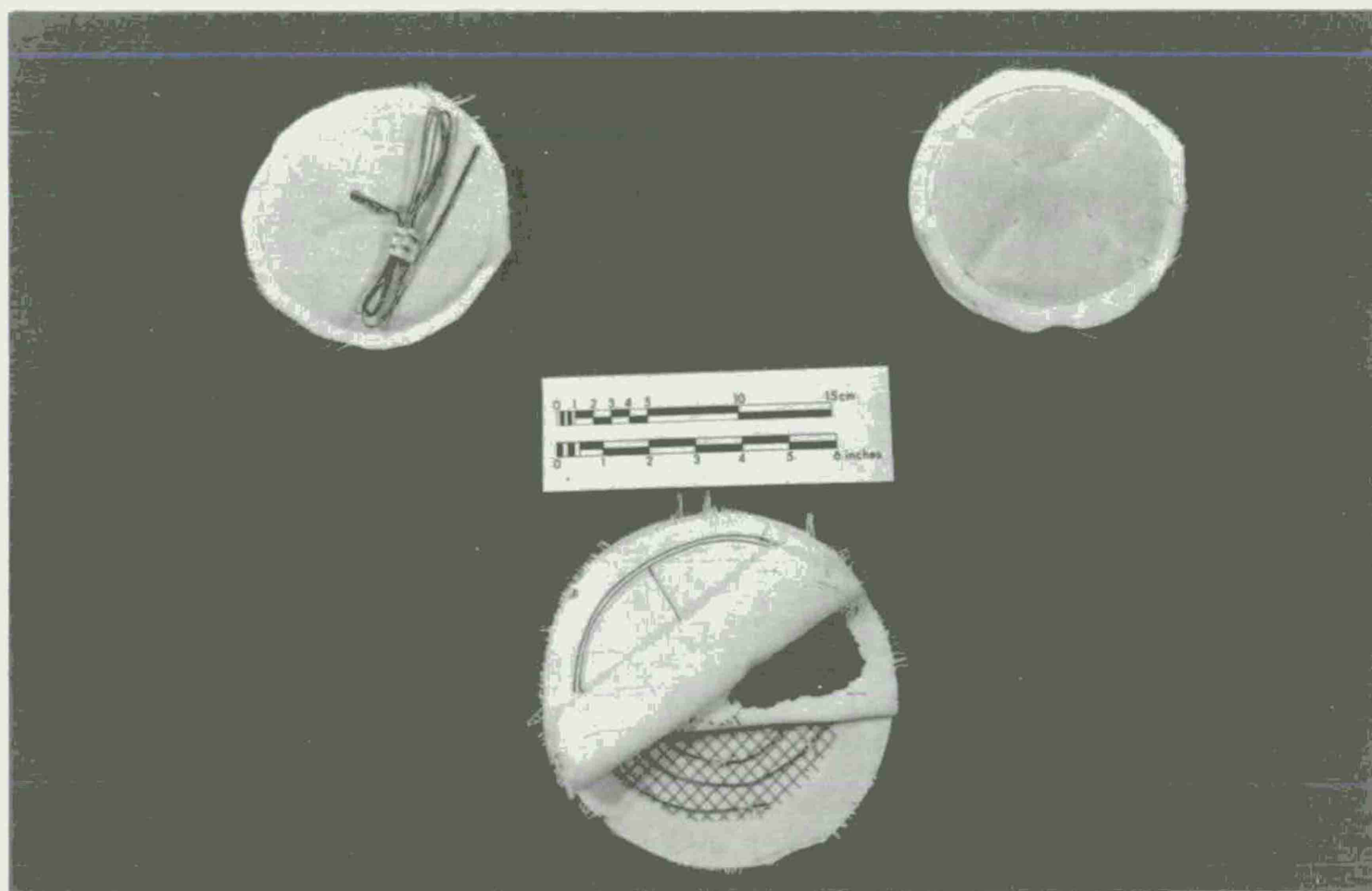


Figure 6. 5-Inch, One-Dimensional Igniter

The unsmoothed experimental pressures from each of the piezoelectric transducers are shown in Figure 7. The time scale is referenced with respect to the instant at which the firing voltage was applied to the electric initiator. The sequence of events, as depicted in these traces, is well-behaved and easily explained in the context of the phenomenology earlier discussed. After the igniter functions at the base of the charge, propellant is locally ignited and an axial, convectively driven pressure front proceeds forward through the propellant bed. At approximately 32 ms, the combustion wave reaches the base of the projectile, stagnates, as revealed by the slope change of the forward curves, and is reflected toward the base of the case. The position of the reflected wave is easily tracked by the reversal of the order of the curves at the higher pressures. Figure 8 provides an alternate representation of these same data, presenting pressure-position profiles in the chamber at selected times. Again, we see a pressure front traveling from the rear, yielding an initial, forward-facing pressure gradient. Arrival of the front at the forward station is seen at about 31.5 ms, and the development of a rear-facing gradient indicates reflection of the wave.

The unsmoothed experimental pressures from each of the strain gages are shown in Figure 9. The strain gages were arbitrarily calibrated by requiring agreement of P2 and S2 (the rearmost sidewall transducers) when 15 MPa was reached at P2. As above, the sequence of events exhibited in these strain measurements is well-behaved, and for the most part reproduces that displayed by the piezoelectric measurements. There is some detail on the S4 trace not seen on the P4 record that is perhaps an indication of solid-phase dynamics. Figure 10 displays these data in the form of "strain-inferred" pressure profiles in the chamber. These curves reproduce the early behavior exhibited by the gas pressure profiles, but significant differences evolve at later times. We note an apparent rarefaction wave traversing the chamber in the vicinity of 33.0-33.5 ms. There is also a more persistent rear-facing pressure gradient here, possibly the result of persistent stresses induced in the forward end of the propellant column during compaction of the bed.

Figure 11 displays a comparison of pressures measured using piezoelectric and strain gages. In our previous work²⁵, we relied solely on strain gages, calibrated as described above, to monitor the pressure in the tube. We see here that while agreement between piezoelectric and strain gages is excellent at the rearmost station, presumably least affected by solid-phase loading, the agreement at the forward end of the case is poor, where the strain record cannot even be used as a reliable indicator of time-of-arrival of the gas pressure pulse.

²⁵T. C. Minor, A. W. Horst and J. K. Kelso, "Experimental Investigation of Ignition-Induced Flow Dynamics in Bagged-Charge Artillery," 15th JANNAF Combustion Meeting, CPIA Publication 297, Vol. I, pp. 61-83, February 1979.

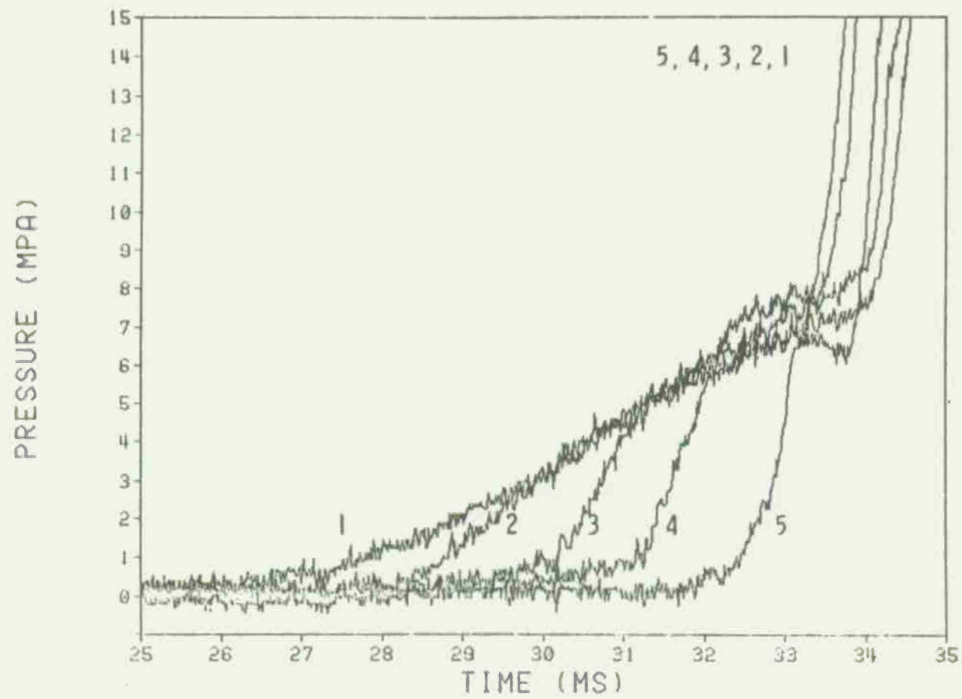


Figure 7. Experimental Piezoelectric Pressures, NOSOL 318 Propellant

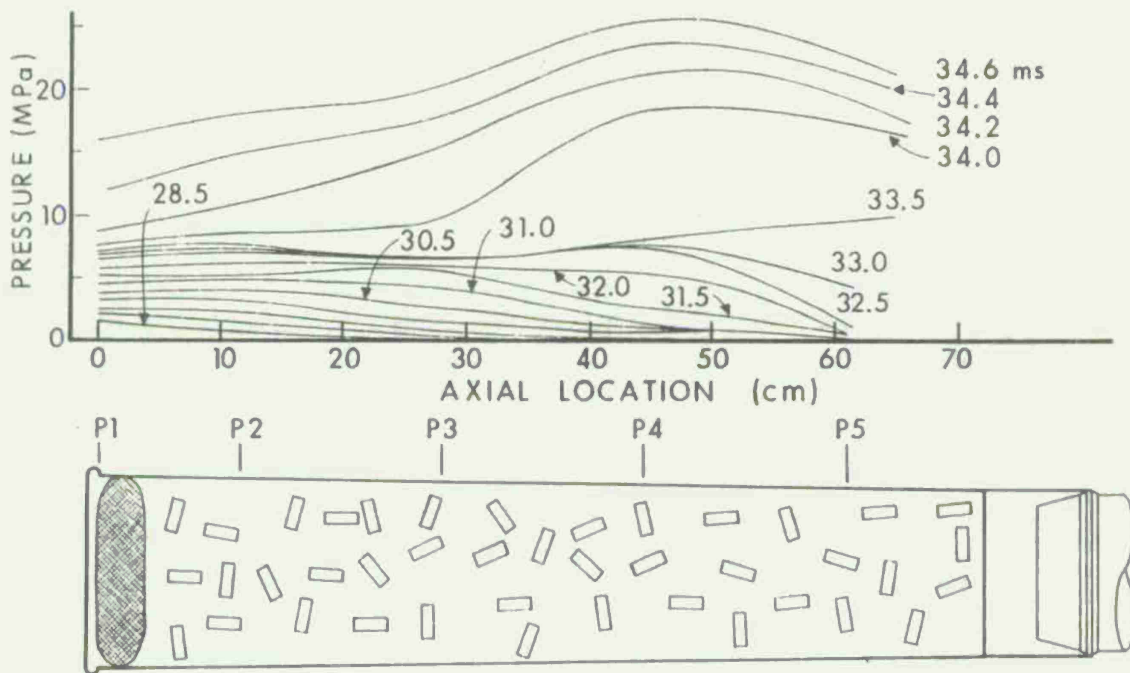


Figure 8. Experimental Piezoelectric Pressure Profiles, NOSOL 318 Propellant

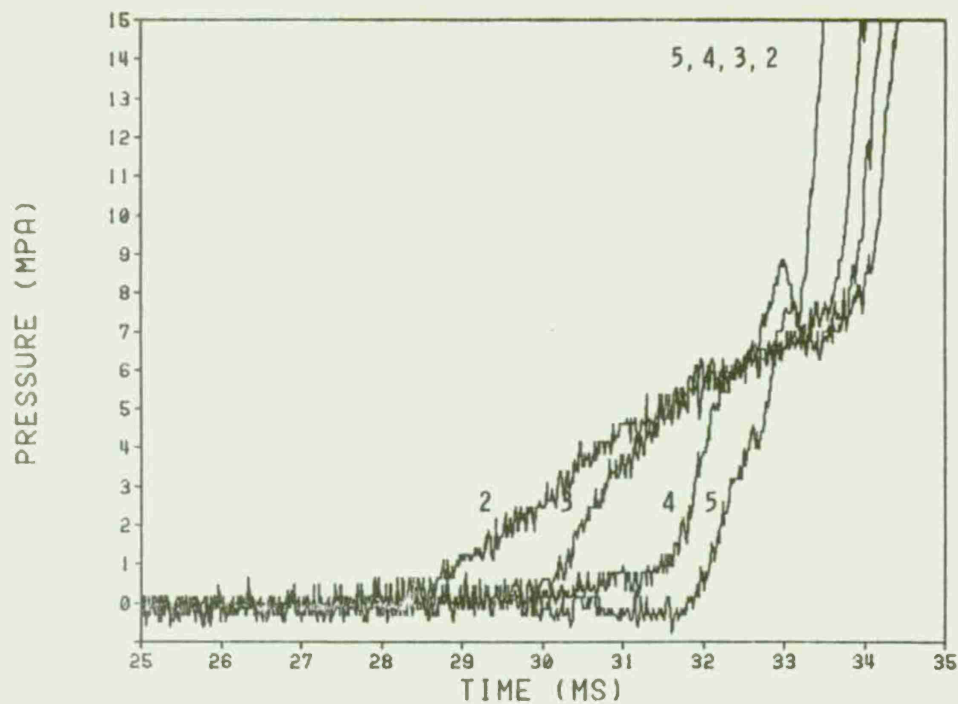


Figure 9. Experimental Strain Pressures, NOSOL 318 Propellant

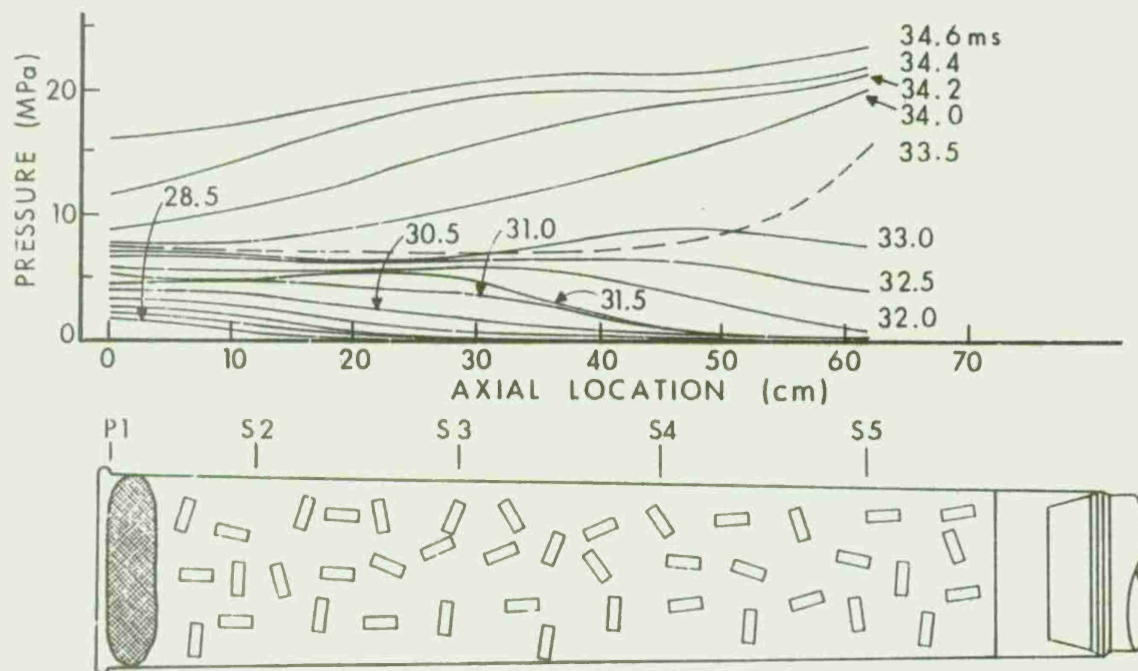


Figure 10. Experimental Strain Pressure Profiles, NOSOL 318 Propellant

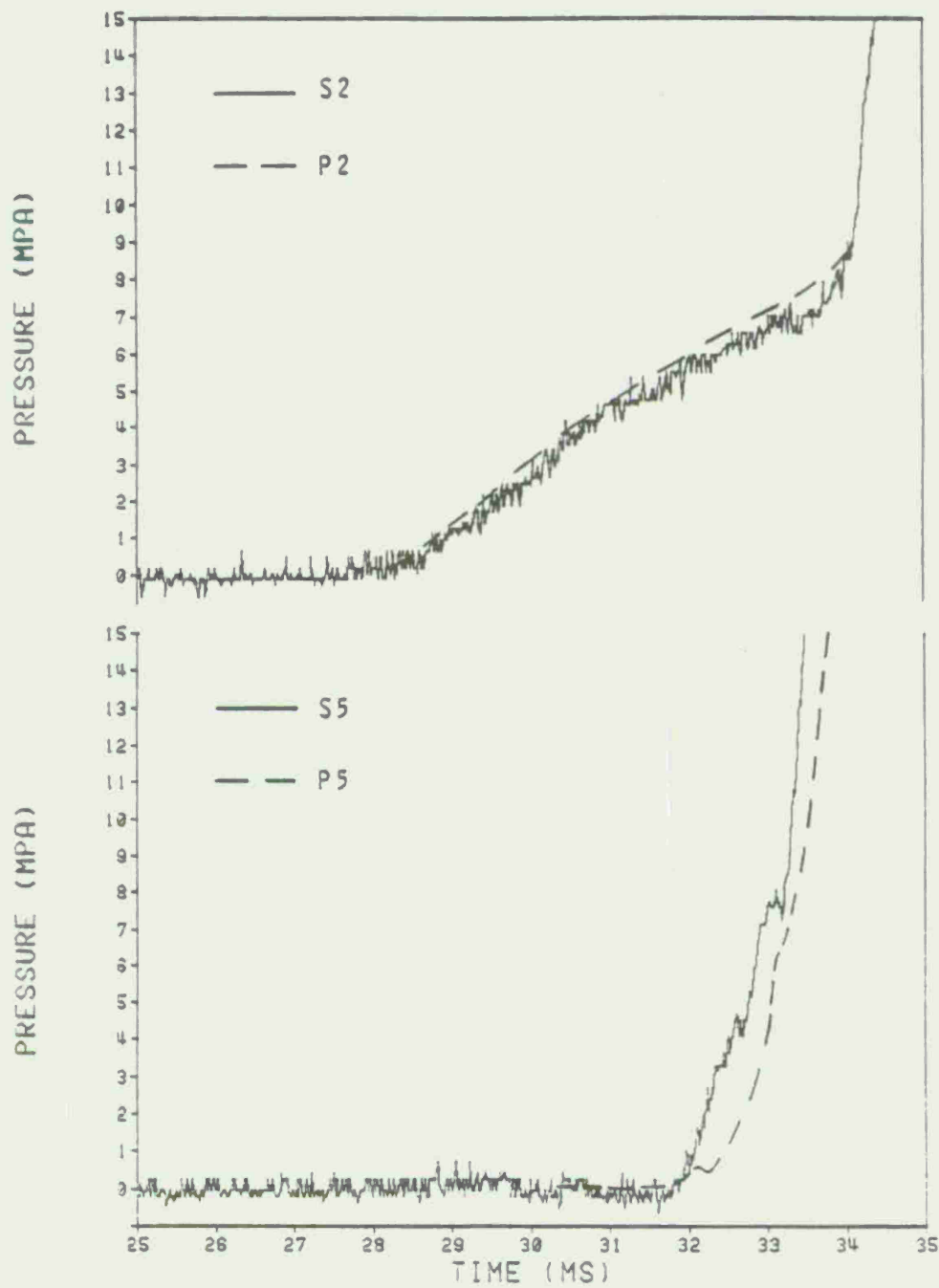


Figure 11. Comparison of Experimental Piezoelectric and Strain Pressures, NOSOL 318 Propellant

NOVA code simulations of the "1-D" NOSOL 318 firings were performed using the input data base provided in Appendix A. Independently determined values for required input parameters were employed wherever possible. Propellant thermochemical properties were calculated using the BLAKE code²⁶, burning rates were based on closed bomb measurements²⁷, and bed rheology was characterized by reference to results from quasi-steady compaction studies²⁸. The propellant ignition temperature was arbitrarily set at 450 K, and the igniter output profile was depicted to be either a simple, constant venting of the appropriate quantity of black powder combustion products or a slightly ramped version of the same (see Figure 12). The total action time of approximately 20 ms was based on the results of some earlier igniter characterization tests, depicted in Figure 13, though no attempt was made to reproduce any of the detailed structure of igniter performance.

Figure 14 provides one comparison of theory with experiment for the first NOSOL firing. Ignition delays are underpredicted with both igniter profiles employed, so a time translation has been introduced to render coincidental the experimental and predicted times for a pressure of 15 MPa at the breech position. Some sensitivity is seen here with respect to the character of the igniter description, suggesting the need for a more careful representation of its temporal output. However, while pressure-front propagation rates are in substantial agreement with experiment, the sharp discontinuity in the pressurization curves, marking the arrival of the reflected wave front, is completely missing in the simulations. Altering propellant bed compaction characteristics (by changing the rate of propagation of an intergranular disturbance, a_0 , as in the packed bed) to approximate more closely measurements made on single-base, solvent-processed propellants is seen in Figure 15 to significantly alter predicted pressure-difference profiles, though little improvement is seen (Figure 14) with respect to the previously described problem.

Figure 16 provides a composite display of predicted and observed pressure-front propagation profiles (based on a level of 1 MPa), and of predicted flame-front propagation. As mentioned before, flamespread data could not be reduced because of the low level of luminosity observed during the firings of NOSOL 318 propellant. Note again the dependence of predicted results on the igniter description.

²⁶E. Freedman, "BLAKE, A Ballistic Thermodynamics Code Based on TIGER," *Proceedings of the International Symposium on Gun Propellants*, Dover, NJ, 1973.

²⁷S. E. Mitchell, "Selected Properties of Navy Gun Propellants," IHSP 76-128, Naval Ordnance Station, Indian Head, MD, January 1976.

²⁸A. W. Horst and F. W. Robbins, "Solid Propellant Gun Interior Ballistics Annual Report: FY76/TQ," IHTR 456, Naval Ordnance Station, Indian Head, MD, January 1977.

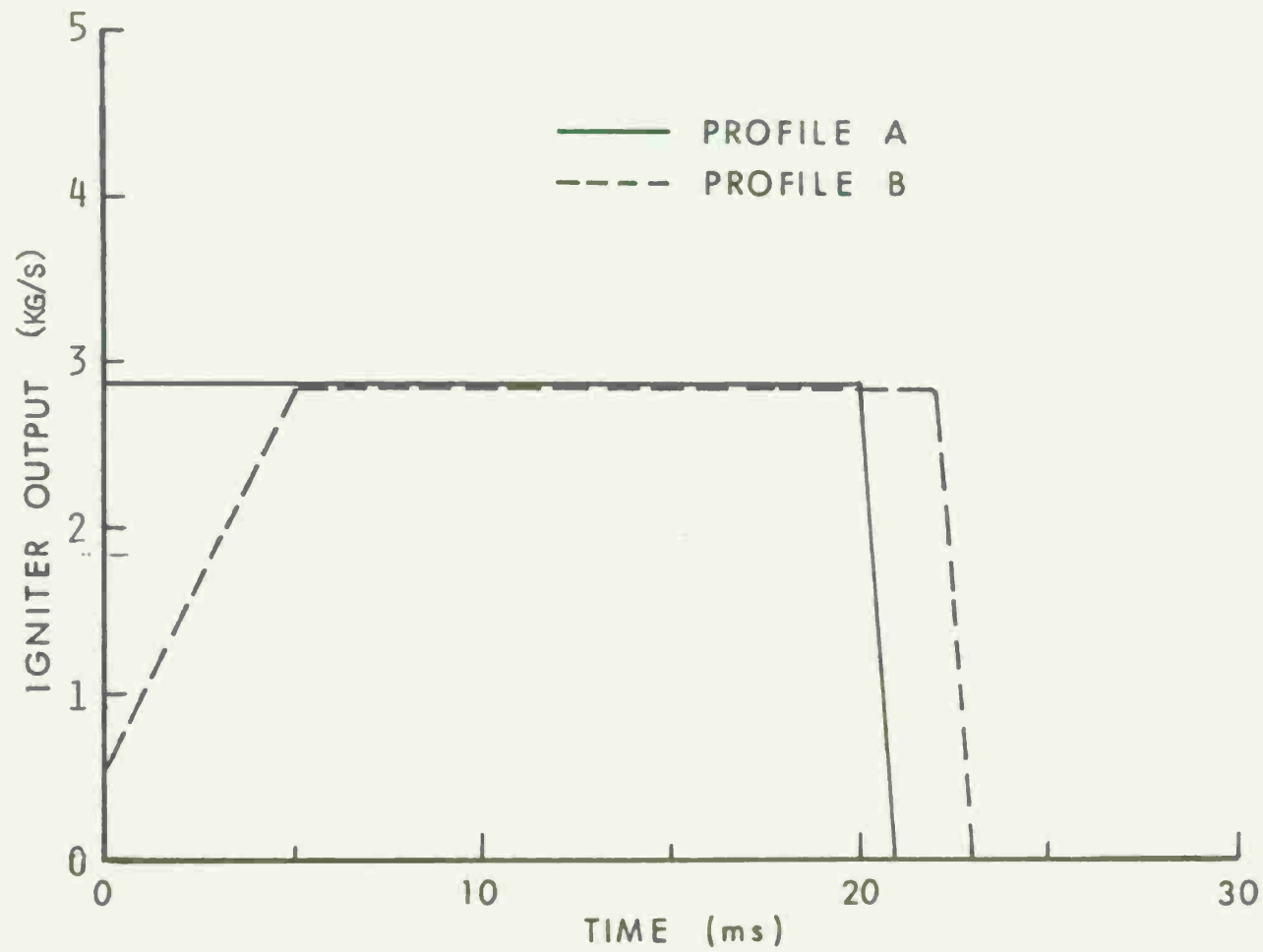


Figure 12. Simplified Igniter Output Profiles (Input to NOVA Code)

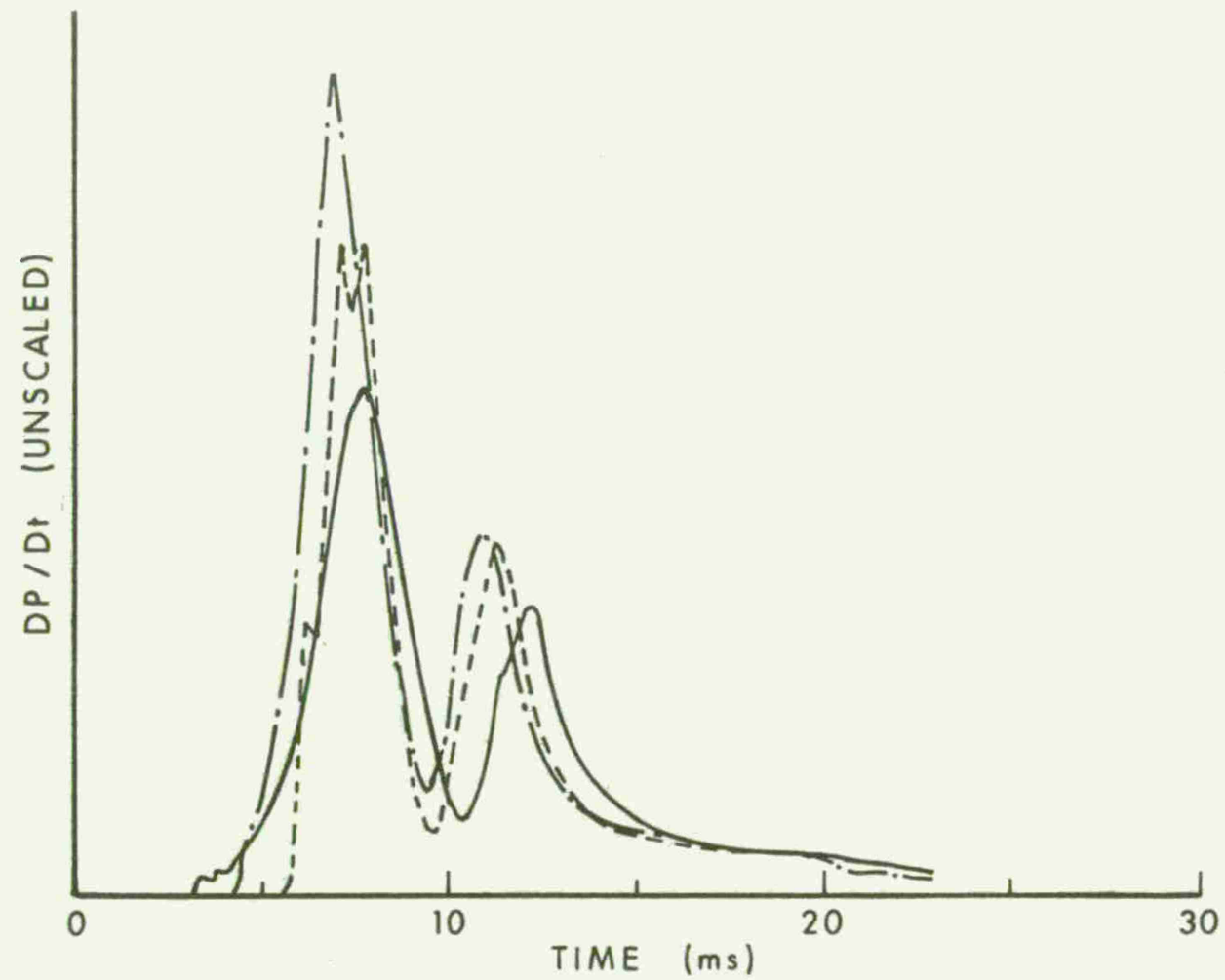


Figure 13. One-Dimensional Igniter Static Firing Results

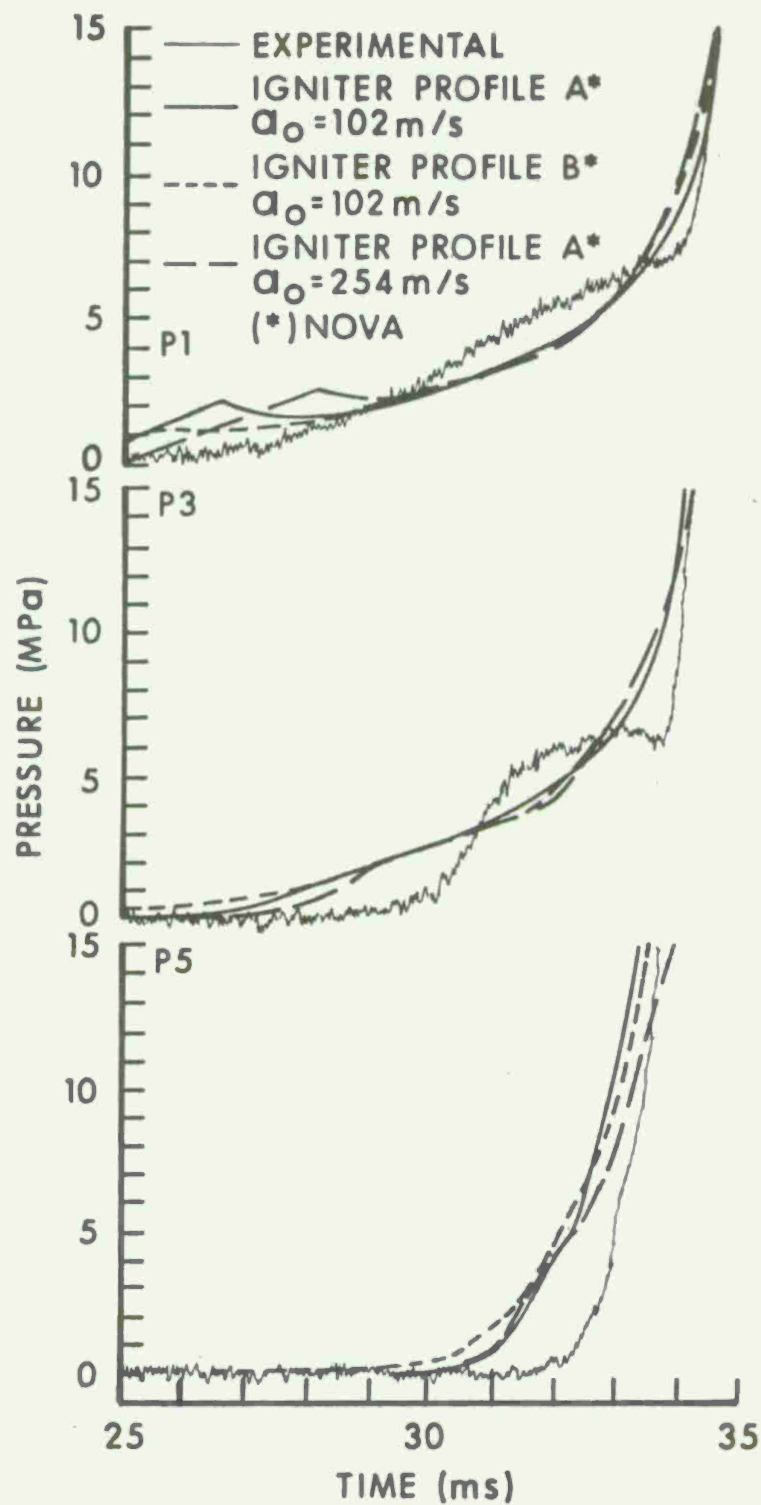


Figure 14. Comparison of Experimental and Calculated Pressures, NOSOL 318 Propellant

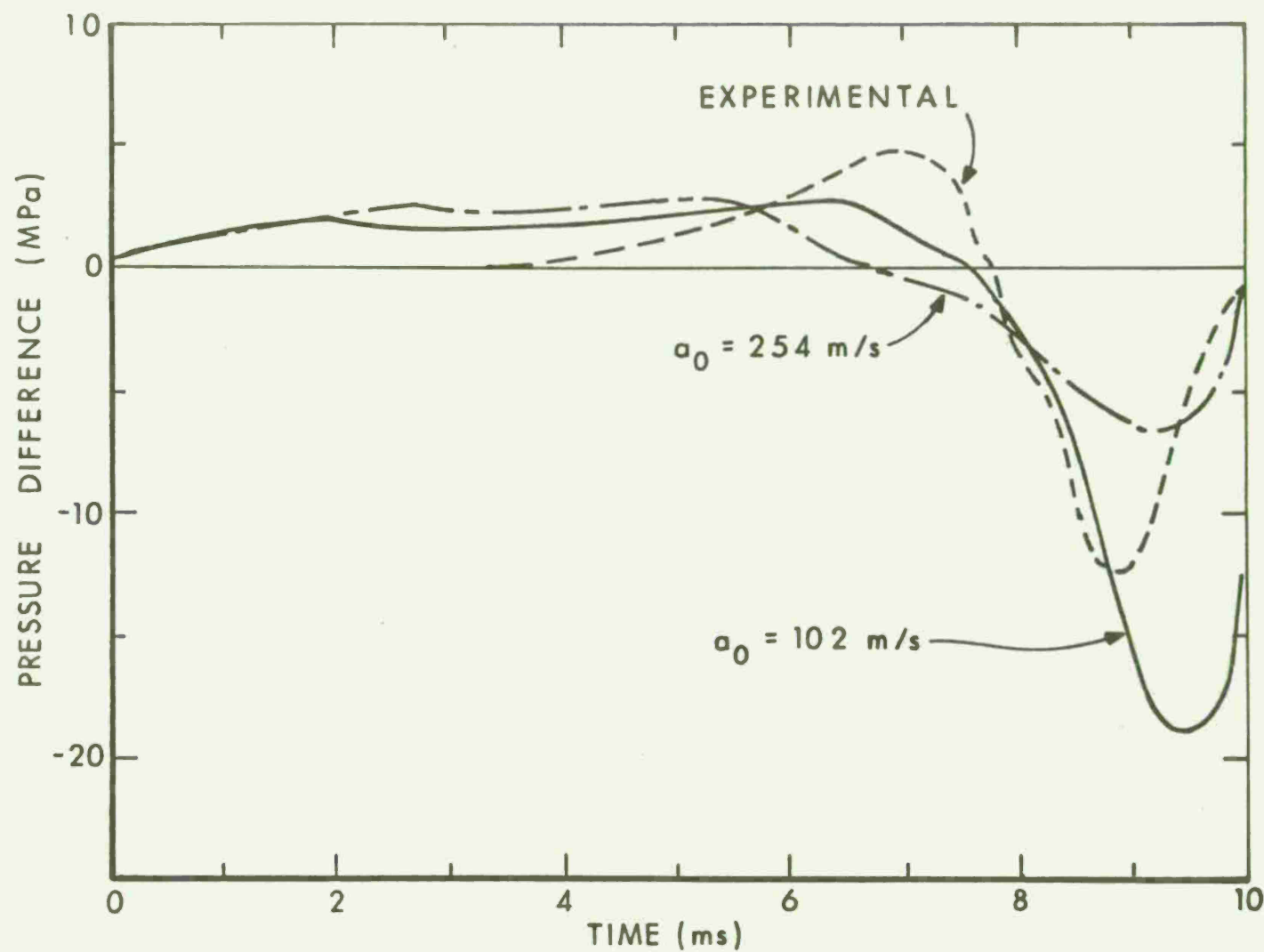


Figure 15. Comparison of Predicted and Experimental Pressure-Difference Profiles (P1-P5) for NOSOL 318

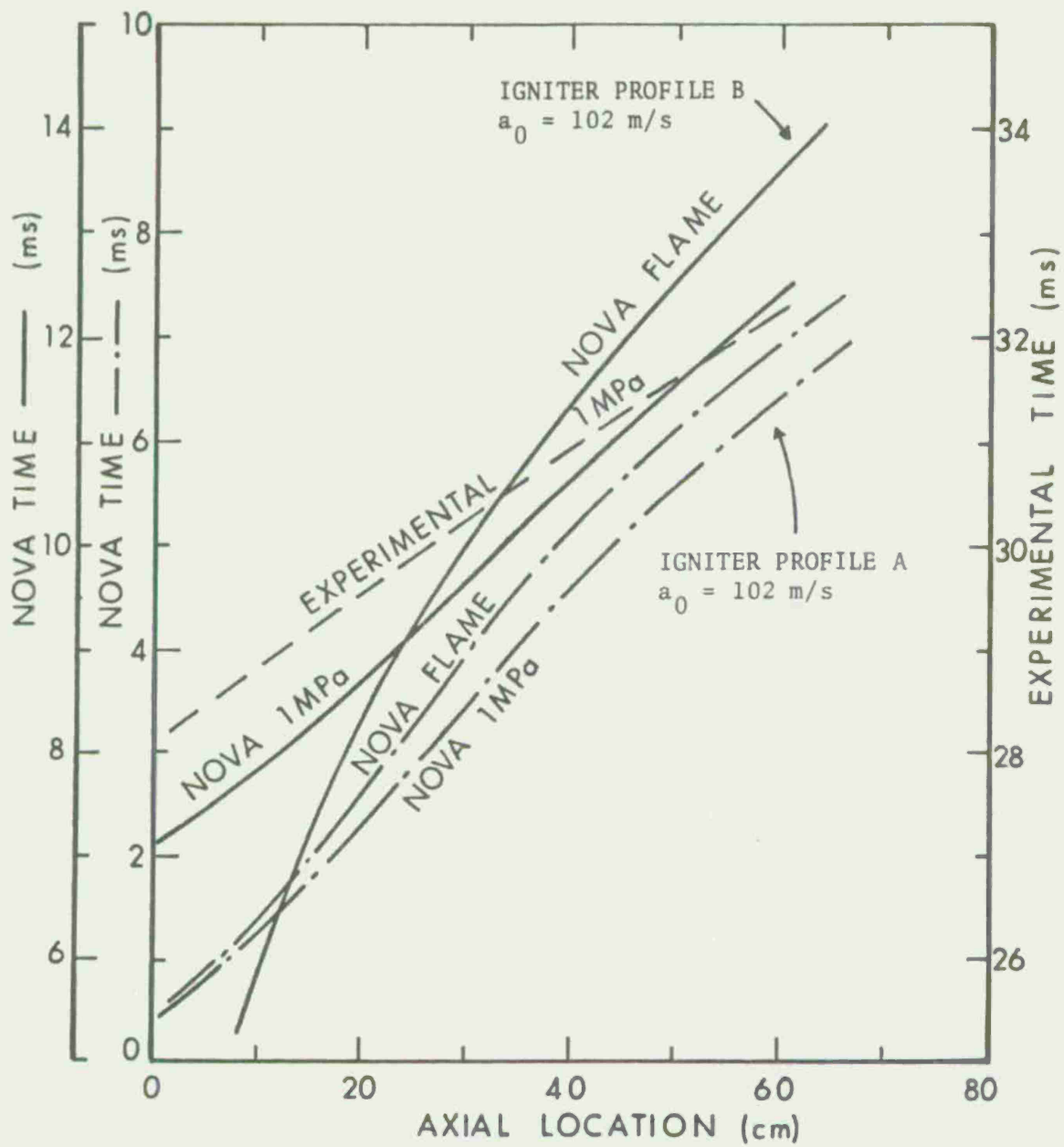


Figure 16. Experimental and Calculated Flame and Pressure Fronts for NOSOL 318 Propellant

B. One-Dimensional, M30A1 Tests

The M30A1 propellant selected for these tests was physically similar to the NOSOL 318 to permit a comparison between the details of the interior ballistic processes for the two. The seven-perforation M30A1 had a length of 24.1 mm, an outer diameter of 10.6 mm, and a perforation diameter of 0.86 mm. The propellant charge mass was 10.07 kg. The initial axial ullage on the shot discussed here in detail was 53 mm, and the projectile did not move during the event. Due to the increased luminosity of the flame for this shot, when compared to that of the NOSOL 318, flamespread data could be visually tracked. As before, only one of the two rounds is reported in detail; the second reproduced these results.

Figure 17 displays the flamespread through the M30A1 propellant at 10,000 frames per second. After a period of diffuse luminosity, with ill-defined flame propagation in the rear part of the charge, the flame proceeds monotonically to the front of the charge.

Unsmoothed, experimental pressure-time profiles as recorded by the piezoelectric transducers are shown in Figure 18. The low-pressure front (~ 1 MPa) is seen to propagate forward in an orderly fashion in much the same manner as in the NOSOL charges. However, the details of the stagnation event are absent here, as rapid pressurization at mid-chamber leads to an early failure of the case. This sequence of events becomes clearer upon examination of Figure 19. We see an extremely rapid pressure buildup near mid-chamber at about 29 ms into the cycle, with virtually no penetration into the forward portion of the charge until after 29.6 ms. One can conjecture that a coupling of the relatively high burning rates of M30A1 propellant at low pressures with local compaction of the bed at the pressure front resulted in a temporary blockage to flow. The interplay of propellant compaction and friction between the propellant bed and the case sidewall could impact significantly on this process.

Figure 20 contains plots of the experimental strain pressures recorded in the M30A1 test. As with the NOSOL example, the strain records substantially reflect the same events as the piezoelectric data, with the exception of some detail on the S5 trace, presumably the result of propellant motion and compaction at the forward end of the case. Figure 21 displays these data as "strain-inferred" pressure profiles, revealing the same general character as the plots of Figure 20. However, the gradient from S4 to S5 is less steep than that from P4 to P5, suggesting once again the presence of a locally severe impedance to gas flow. Figure 22 compares the piezoelectric and strain pressures at rear and forward locations along the case. It appears that a low-level stress wave is transmitted through the relatively stiff M30A1 propellant bed, reaching the forward end of the case before the gas-pressure front arrives.

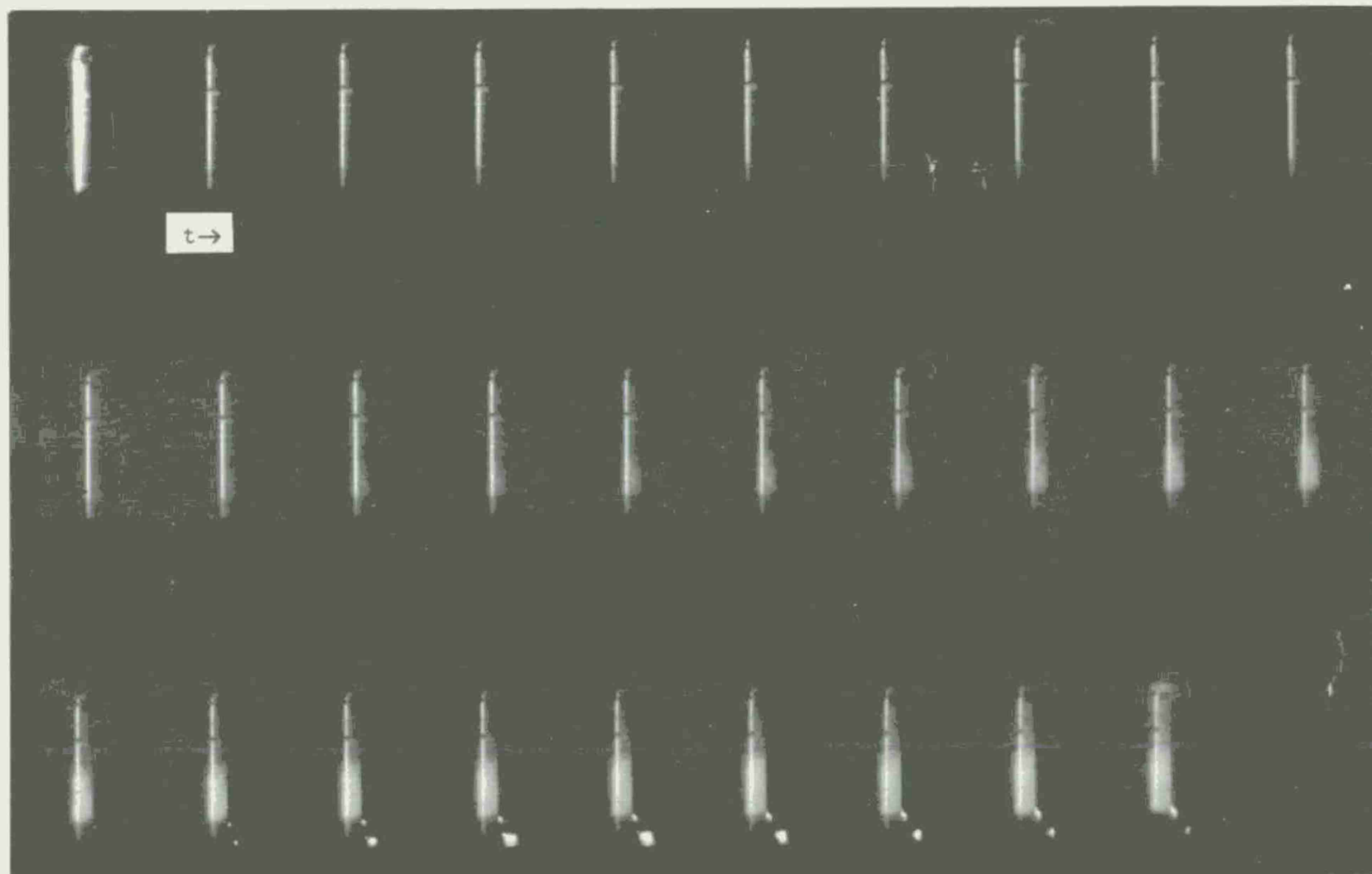


Figure 17. Flamespread, M30A1 Propellant

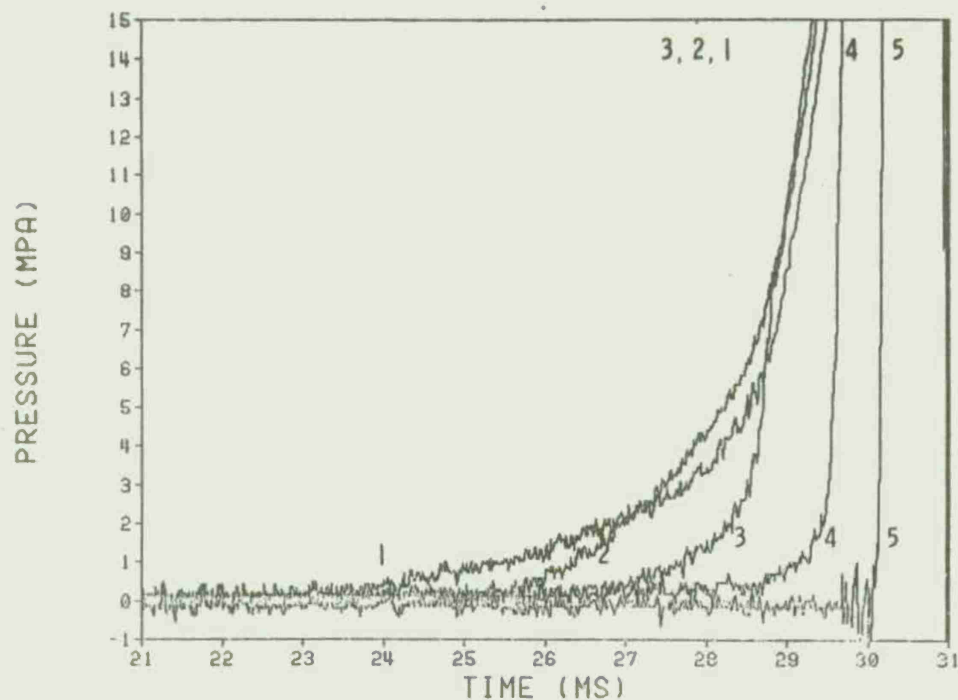


Figure 18. Experimental Piezoelectric Pressures, M30A1 Propellant

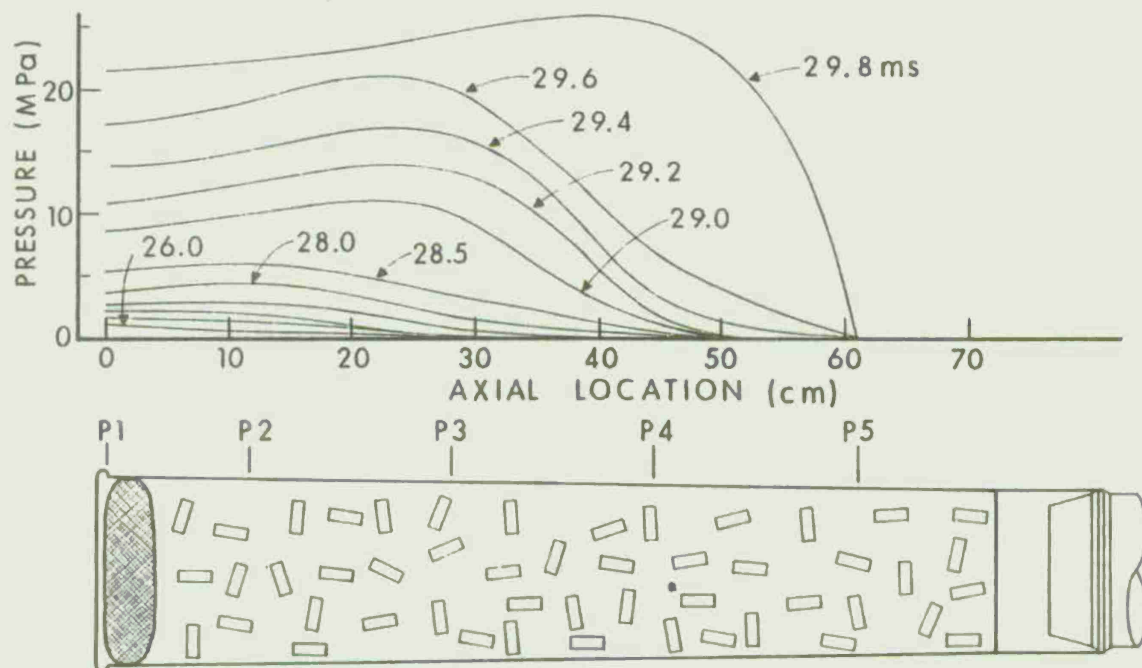


Figure 19. Experimental Piezoelectric Pressure Profiles, M30A1 Propellant

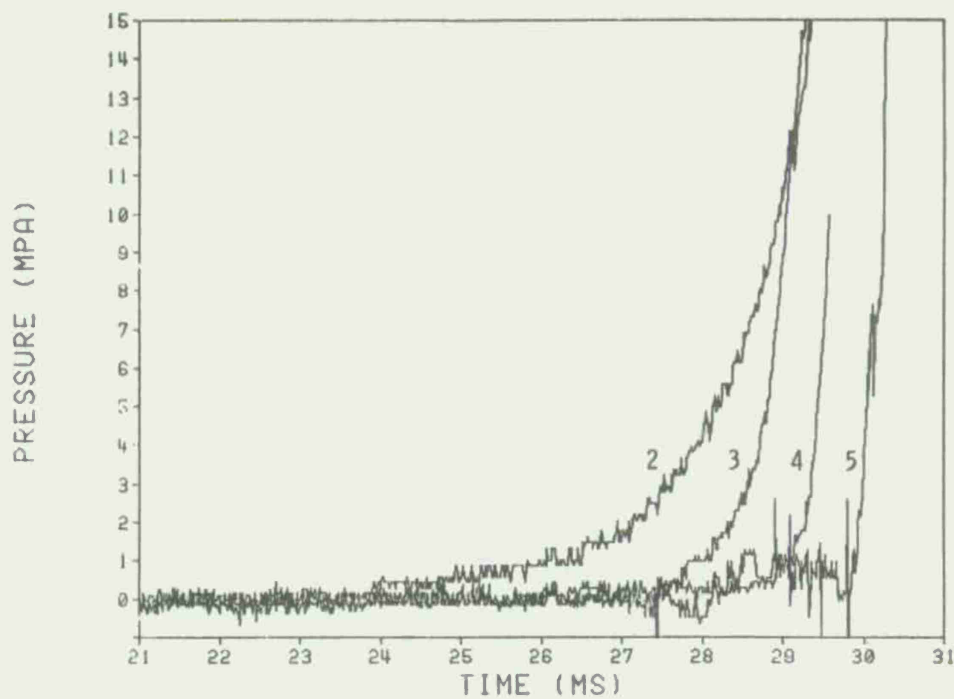


Figure 20. Experimental Strain Pressures, M30A1 Propellant

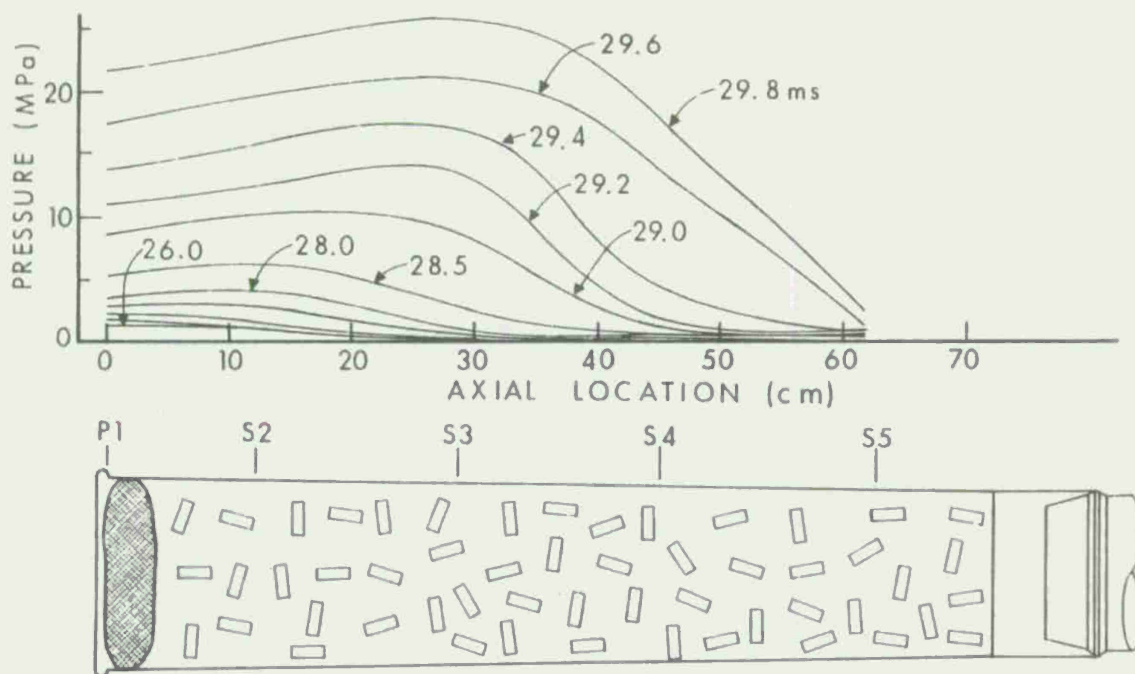


Figure 21. Experimental Strain Pressure Profiles, M30A1 Propellant

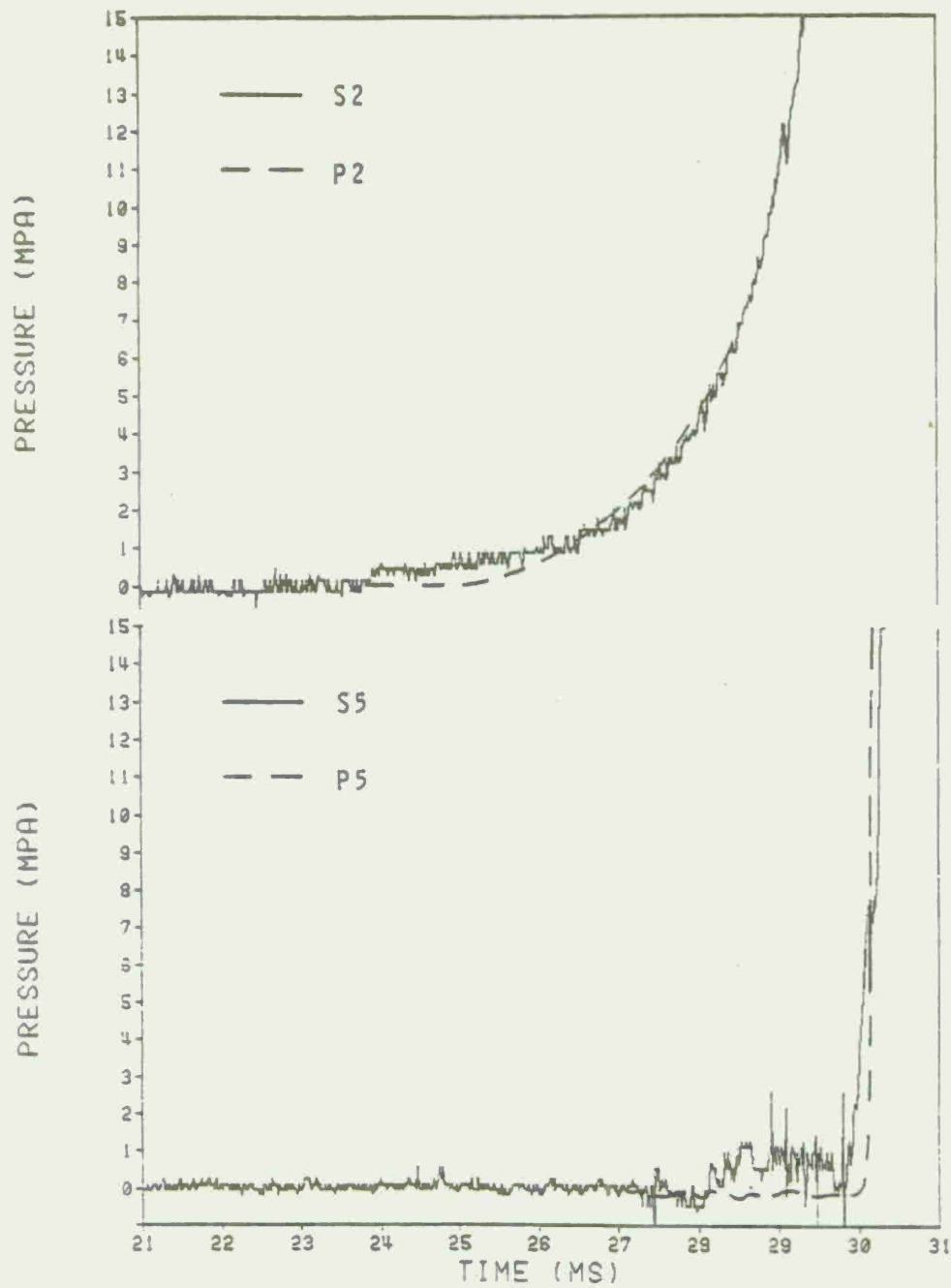


Figure 22. Comparison of Experimental Piezoelectric and Strain Pressures, M30A1 Propellant

Comparisons of NOVA predictions (using the data base of Appendix B) to experimental results for M30A1 propellant are provided in Figures 23 and 24. Simulation of the low-pressure (< 5 MPa) regime is seen in Figure 23 to be no more satisfactory than for the NOSOL firings. While a comparison at the time of stagnation is not possible because of case failure prior to that event, any agreement at that time would be fortuitous, because of a failure to simulate the apparent choking of flow near mid-chamber earlier in the cycle.

Figure 24 depicts a comparison between the model predictions for flame- and pressure-front propagation through the charge. The experimental flamespread plot reflects the events shown in Figure 17, that is, a region of poorly defined movement followed by the customary monotonic flame front. During the well-behaved portion of the cycle, the simulations are in excellent agreement with the experimental flamespread rate. However, over the range of input variables studied, we have not obtained an accurate simulation of the transit of the low-amplitude pressure front through the bed, again possibly because of poorly understood bed rheology and wall interactions not considered in the model.

IV. CONCLUSIONS

We have provided experimental data which can be used in assessing the relative merits of existing one-dimensional, unsteady, two-phase flow interior ballistic models. A full-scale comparison of the models, exercised using standardized, independently determined, input parameters, has not yet been accomplished. However, a comparison of experimental results to sample calculations using an existing model has served to suggest several areas of concern to modelers and experimental investigators alike. First, the sensitivity of early time predictions of flow to igniter description and the lack of overall agreement between theory and experiment for this early portion of the cycle should be of concern to all. Certainly, a more careful experimental characterization of igniter performance is required. The problem may reach also to the inadequacy of the treatment of the overall ignition process itself in many of the codes. The diffuse nature of the experimentally observed flame development in the rear of the M30A1 charges suggests anything but a sharply defined, convectively driven flame front. Treatment of low-pressure ignition systems may well require recognition of a far more complicated sequence of events, perhaps involving some important gas-phase reactions, leading to full, "steady-state" combustion.

Further, we have noted the sensitivity of predicted results to our description of propellant bed rheology, as influenced in the NOVA code by selection of a value for the speed of propagation of a small disturbance in the packed bed. This quantity is typically the result of an indirect measurement, often being deduced from quasi-steady propellant bed compaction characteristics. We also point out that use of what are

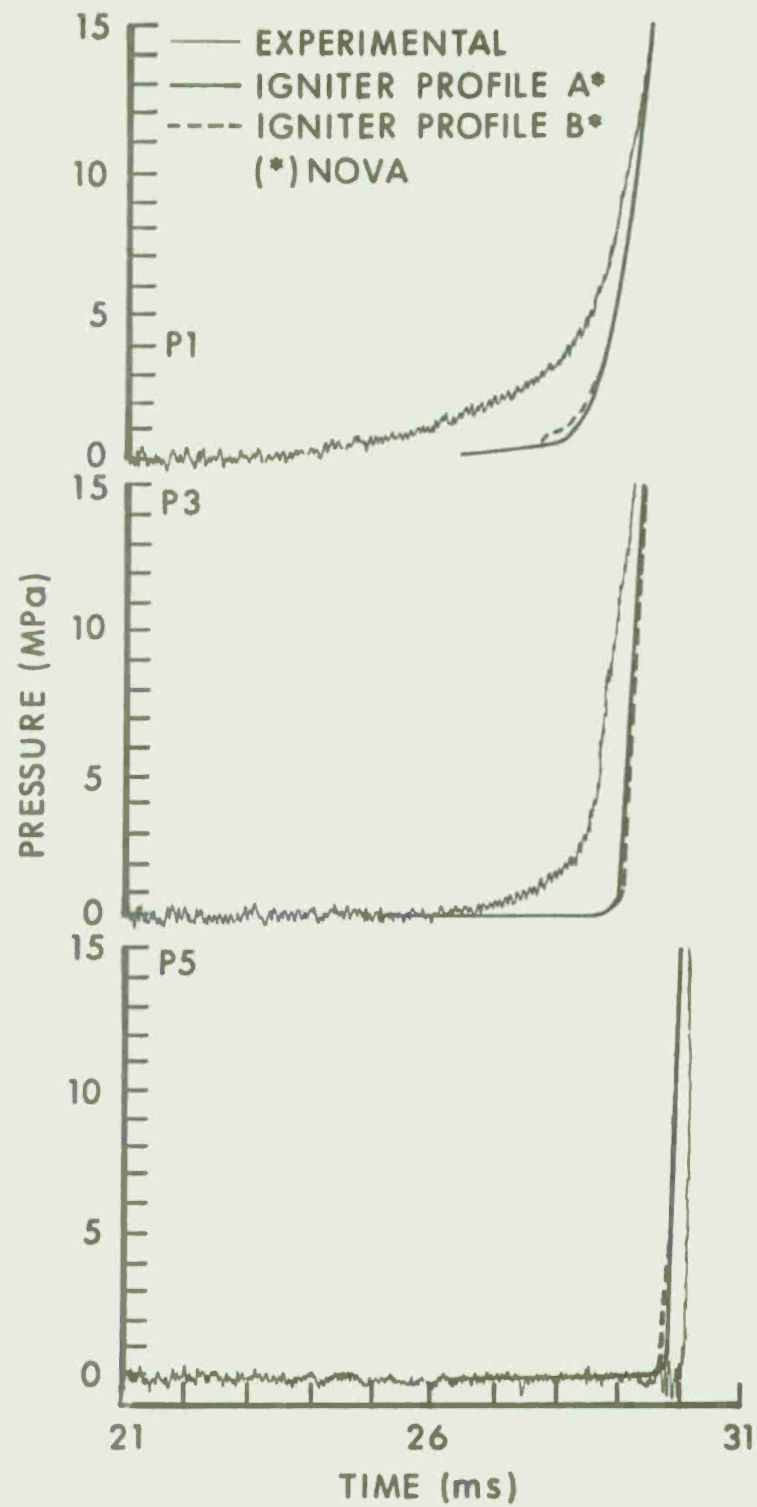


Figure 23. Comparison of Experimental and Calculated Pressures, M30A1 Propellant

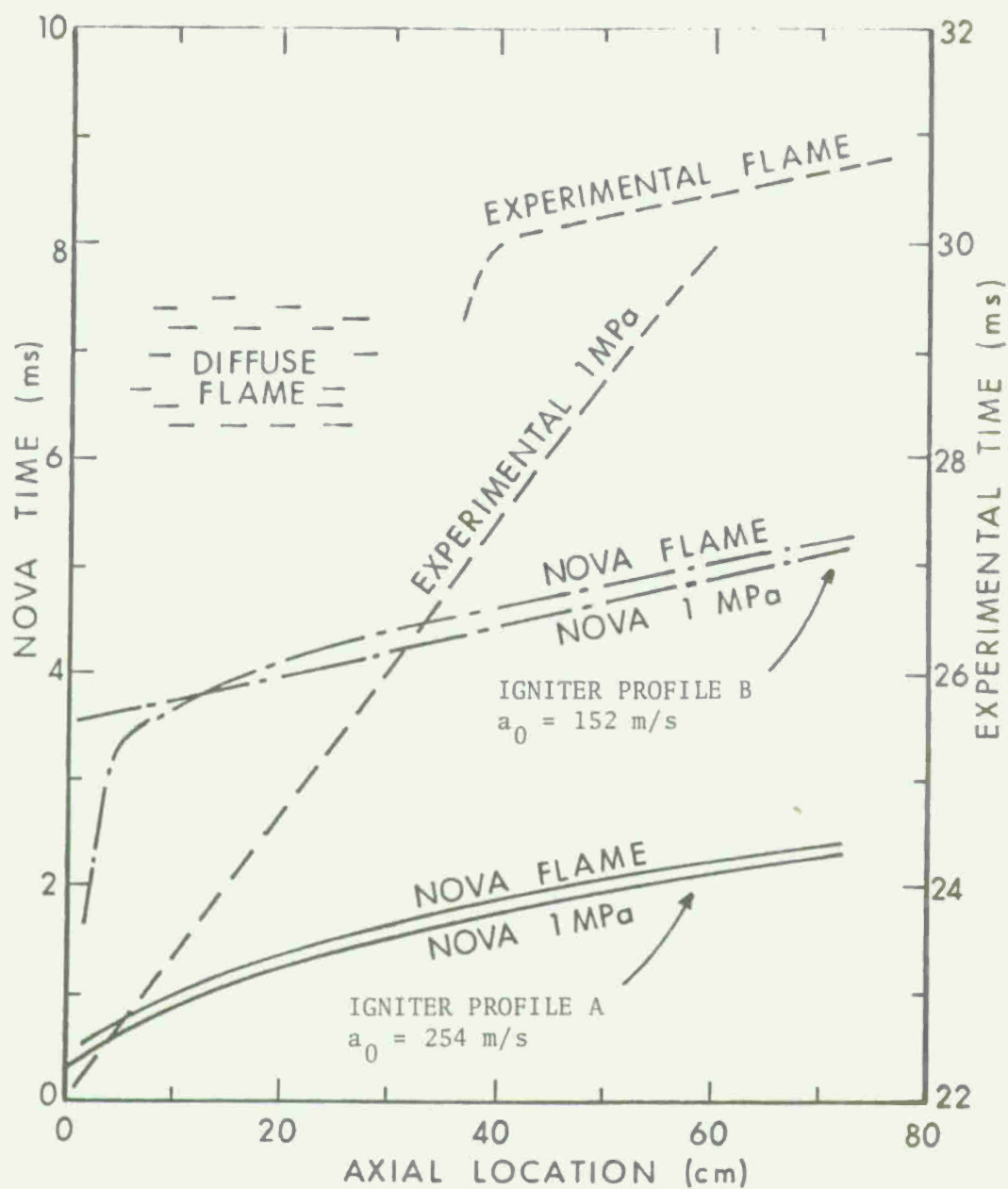


Figure 24. Experimental and Calculated Flame and Pressure Fronts for M30A1 Propellant

believed to be extreme values for this parameter offers little promise for effecting, within the framework of the current representation, a satisfactory simulation of observed, sharp discontinuities in the slopes of pressure-time profiles as the reflected wave passes.

Numerous other features of the flamespread process have not been addressed in this exercise, but are certainly worthy of further attention. Low-pressure propellant burning rates, often not well characterized, will be extremely influential in determining the progress of a convectively driven flame front. The corresponding resistance to flow offered by the propellant bed, and as influenced by bed compaction and interaction with the wall, will be equally important. Modelers and experimentalists will have to continue to work hand in hand to effect improvement in such areas, required for one-dimensional and multi-dimensional models alike.

ACKNOWLEDGMENTS

The authors are grateful to Dr. J. L. East, Dr. J. L. Johndrow, Mr. W. R. Burrell and many other individuals at the Naval Surface Weapons Center, Dahlgren, VA for arranging and conducting the experimental work reported here. Also, the assistance of Dr. K. J. White and Mr. J. R. Kelso in the manufacture and testing of experimental ignition systems is sincerely appreciated.

REFERENCES

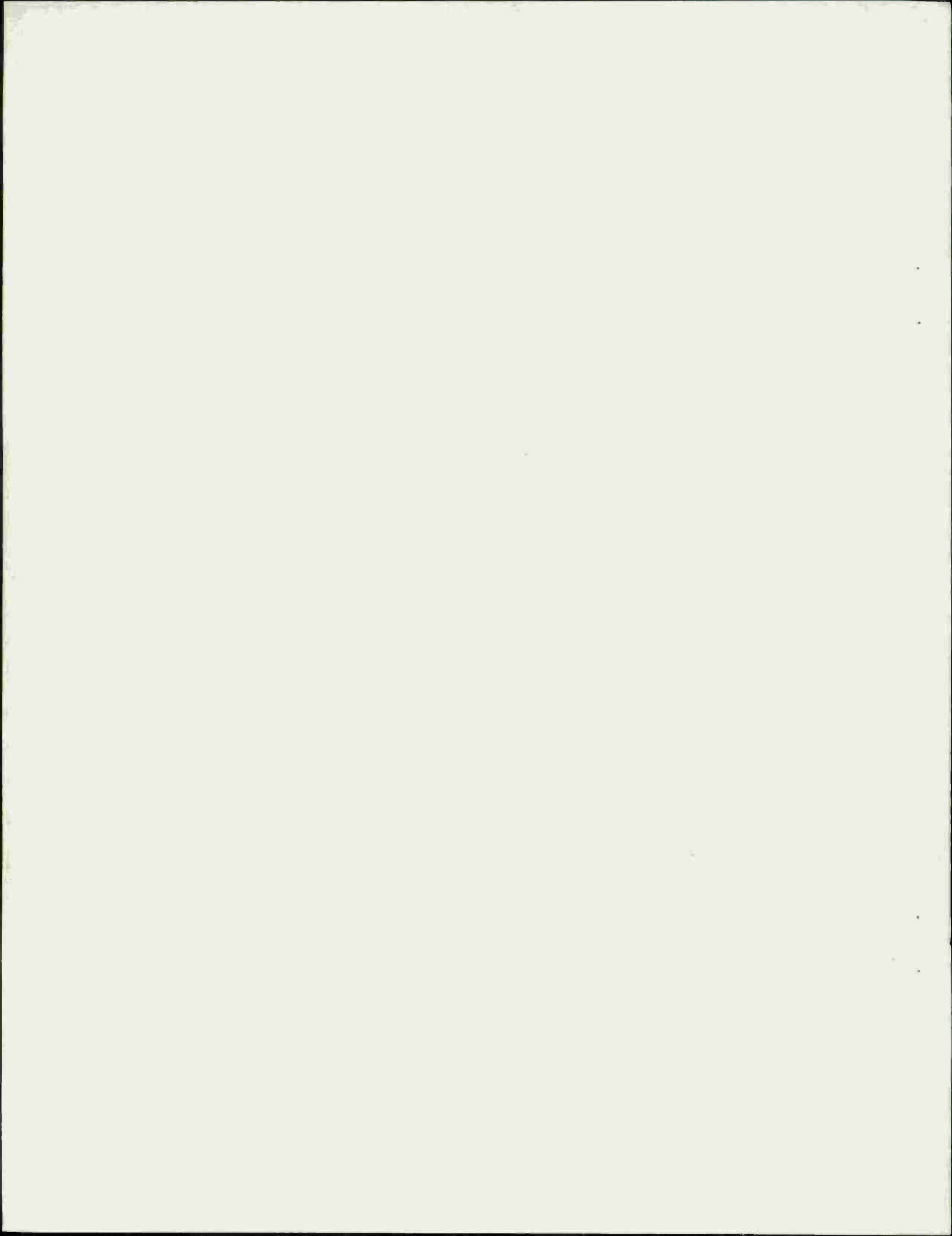
1. P. G. Baer and J. M. Frankle, "The Simulation of Interior Ballistic Performance of Guns by Digital Computer Program," Report 1183, Ballistic Research Laboratories, Aberdeen Proving Ground, MD, December 1961. (AD #299980)
2. A. W. Horst, I. W. May, and E. V. Clarke, "The Missing Link Between Pressure Waves and Breechblows," 14th JANNAF Combustion Meeting, CPIA Publication 292, Vol. II, pp. 277-292, December 1977.
3. J. Chandra and C. Zoltani, "Proceedings of ARO Workshop on Multi-phase Flows," US Army Research Office and the Ballistic Research Laboratory, Aberdeen Proving Ground, MD, February 1978.
4. K. K. Kuo, "A Summary of the JANNAF Workshop on Theoretical Modeling and Experimental Measurements of the Combustion and Fluid Flow Processes in Gun Propellant Charges," 13th JANNAF Combustion Meeting, CPIA Publication 281, Vol. I, pp. 213-233, December 1976.
5. E. B. Fisher, "Quality Control of Continuously Produced Gun Propellant," Calspan Report No. SA-5913-X-1, Calspan Corporation, Buffalo, NY, August 1977.
6. E. B. Fisher, "Investigation of Breechblow Phenomenology," Contract Report ARBRL-CR-00412, Ballistic Research Laboratory, USA ARRADCOM, Aberdeen Proving Ground, MD, January 1980. (AD #B046080L)
7. P. S. Gough and F. J. Zwarts, "Some Fundamental Aspects of the Digital Simulation of Convective Burning in Porous Beds," AIAA/SAE 13th Propulsion Conference, AIAA Paper No. 77-855, July 1977.
8. P. S. Gough, "Theoretical Study of Two-Phase Flow Associated with Granular Bag Charges," Contract Report ARBRL-CR-00381, Ballistic Research Laboratory, USA ARRADCOM, Aberdeen Proving Ground, MD, September 1978. (AD #A062144)
9. P. S. Gough, "Two-Dimensional Convective Flamespreading in Packed Beds of Granular Propellant," Contract Report ARBRL-CR-00404, Ballistic Research Laboratory, USA ARRADCOM, Aberdeen Proving Ground, MD, July 1979. (AD #A075326)
10. K. K. Kuo and J. H. Koo, "Transient Combustion in Granular Propellant Propellant Beds, Part 1: Theoretical Modeling and Numerical Solution of Transient Combustion Processes in Mobile Granular Propellant Beds," Contract Report No. 346, Ballistic Research Laboratory, USA ARRADCOM, Aberdeen Proving Ground, MD, August 1977. (AD #A044998)

REFERENCES (Continued)

11. H. J. Gibeling, R. C. Buggeln and H. McDonald, "Development of a Two-Dimensional Implicit Interior Ballistics Code," Contract Report ARBRL-CR-00411, Ballistic Research Laboratory, USA ARRADCOM, Aberdeen Proving Ground, MD, January 1980. (AD #A084092)
12. A. C. Buckingham, "Modeling Additive and Hostile Particulate Influences in Gun Combustion Turbulent Erosion," 16th JANNAF Combustion Meeting, CPIA Publication 308, Vol. I, pp. 673-690, December 1979.
13. P. S. Gough and F. J. Zwarts, "Theoretical Model for Ignition of Gun Propellant," SRC-R-67, Space Research Corporation, North Troy, VT, December 1972.
14. P. S. Gough, "Fundamental Investigation of the Interior Ballistics of Guns: Final Report," IHCR 74-1, Naval Ordnance Station, Indian Head, MD, August 1974.
15. P. S. Gough, "Computer Modeling of Interior Ballistics," IHCR 75-3, Naval Ordnance Station, Indian Head, MD, October 1975.
16. P. S. Gough, "Numerical Analysis of a Two-Phase Flow with Explicit Internal Boundaries," IHCR 77-5, Naval Ordnance Station, Indian Head, MD, April 1977.
17. S. Ergun, "Fluid Flow Through Packed Columns," Chem. Eng. Progr., Vol. 48, pp. 89-95, 1952.
18. K. E. B. Andersson, "Pressure Drop in Ideal Fluidization," Chem. Eng. Sci., Vol. 15, pp. 276-297, 1961.
19. W. H. Denton, "General Discussion on Heat Transfer," Inst. Mech. Eng. and Am. Soc. Mech. Eng., London, 1951.
20. N. I. Gelperin and V. G. Einstein, "Heat Transfer in Fluidized Beds," Fluidization, edited by J. F. Davidson and D. Harrison, Academic Press, 1971.
21. R. W. MacCormack, "The Effects of Viscosity in Hypervelocity Impact Cratering," AIAA Paper No. 69-354, AIAA Aerospace Science Meeting, 1969.
22. J. L. East, "Experimental Techniques for Investigating the Start-Up Ignition/Combustion Transients in Full-Scale Charge Assemblies," 11th JANNAF Combustion Meeting, CPIA Publication 261, Vol. I, pp. 119-139, December 1974.

REFERENCES (Continued)

23. J. L. East and D. R. McClure, "Experimental Studies of Ignition and Combustion in Naval Guns," 12th JANNAF Combustion Meeting, CPIA Publication 273, Vol. I, pp. 221-257, December 1975.
24. W. R. Burrell and J. L. East, "Effects of Production Packing Depth and Ignition Techniques on Propelling Charge Reaction and Projectile Response," NSWC/DL TR-3705, Naval Surface Weapons Center, Dahlgren, VA, April 1978.
25. T. C. Minor, A. W. Horst and J. K. Kelso, "Experimental Investigation of Ignition-Induced Flow Dynamics in Bagged-Charge Artillery," 15th JANNAF Combustion Meeting, CPIA Publication 297, Vol. I, pp. 61-83, February 1979.
26. E. Freedman, "BLAKE, A Ballistic Thermodynamics Code Based on TIGER," Proceedings of the International Symposium on Gun Propellants, Dover, NJ, 1973.
27. S. E. Mitchell, "Selected Properties of Navy Gun Propellants," IHSP 76-128, Naval Ordnance Station, Indian Head, MD, January 1976.
28. A. W. Horst and F. W. Robbins, "Solid Propellant Gun Interior Ballistics Annual Report: FY76/TQ," IHTR 456, Naval Ordnance Station, Indian Head, MD, January 1977.



APPENDIX A

NOVA CODE INPUT
1-D CHARGE - NOSOL 318

1-D CHARGE NOSOL 318 (HORSTA)

CONTROL DATA

LOGICAL VARIABLES:

PRINT 1 GRAPH 2 DISK WRITE 0 DISK READ 0
 I.R. TABLE 1 FLAME TABLE 1 PRESSURE TABLE(S) 1
 EXOSIVE EFFECT 0 DYNAMIC EFFECT 0 WALL TEMPERATURE CALCULATION 0
 LEFT HAND BOUNDARY CONDITION 0 RIGHT HAND BOUNDARY CONDITION 0 LEFT HAND RESERVOIR 0
 RIGHT HAND RESERVOIR 0 BED PRECOMPRESSED 0
 HEAT LOSS CALCULATION 0 INSULATING LAYER 0

BORE RESISTANCE FUNCTION 1

INTEGRATION PARAMETERS

NUMBER OF STATIONS AT WHICH DATA ARE STORED	35
NUMBER OF STEPS BEFORE LOGOUT	25
TIME STEP FOR DISK START	0
NUMBER OF STEPS FOR TERMINATION	700
TIME FOR TERMINATION (SEC)	.2000E-01
PROJECTILE TRAVEL FOR TERMINATION (INS)	200.00
MAXIMUM TIME STEP (SEC)	.1000E-03
STABILITY SAFETY FACTOR	2.00
SOURCE STABILITY FACTOR	.0500
SPATIAL RESOLUTION FACTOR	.0100
TIME INTERVAL FOR I.R. TABLE STORAGE(SEC)	.1000E-03
TIME INTERVAL FOR PRESSURE TABLE STORAGE (SEC)	.1000E-03

FILE COUNTERS

NUMBER OF STATIONS TO SPECIFY TUBE RADIUS	3
NUMBER OF TIMES TO SPECIFY PRIMER DISCHARGE	3
NUMBER OF POSITIONS TO SPECIFY PRIMER DISCHARGE	3
NUMBER OF ENTRIES IN BORE RESISTANCE TABLE	2
NUMBER OF ENTRIES IN WALL TEMPERATURE TABLE	0
NUMBER OF ENTRIES IN FILLER ELEMENT TABLE	0
NUMBER OF TYPES OF PROPELLANTS	1
NUMBER OF BURN RATE DATA SETS	1
NUMBER OF ENTRIES IN VOID FRACTION TABLE(S)	0 0 0
NUMBER OF ENTRIES IN PRESSURE HISTORY TABLES	5
NUMBER OF ENTRIES IN LEFT BOUNDARY SOURCE TABLE	0
NUMBER OF ENTRIES IN RIGHT BOUNDARY SOURCE TABLE	0
NUMBER OF WALL STATIONS FOR INVARIANT EMBEDDING	0
NUMBER OF BED STATIONS FOR INVARIANT EMBEDDING	0
FRICTION COEFFICIENT	1.0

GENERAL PROPERTIES OF INITIAL AMBIENT GAS

INITIAL TEMPERATURE (DEG.R)	530.0
INITIAL PRESSURE (PSI)	14.7
MOLECULAR WEIGHT (LBM/LBMOL)	29.000
RATIO OF SPECIFIC HEATS	1.4000

GENERAL PROPERTIES OF PROPELLANT BED

INITIAL TEMPERATURE (DEG.R)	530.0
VIRTUAL MASS CONSTANT (-)	0.000
VOID FRACTION PACKING COEFFICIENTS	0.0000 0.0000 0.0000

PROPERTIES OF PROPELLANT 1

PROPELLANT TYPE	NOSOL 318
MASS OF PROPELLANT (LBM)	20.4300
DENSITY OF PROPELLANT (LBM/IN**3)	.0550
FORM FUNCTION INDICATOR	7
OUTSIDE DIAMETER (INS)	.4550
INSIDE DIAMETER (INS)	.0330
LENGTH (INS)	.9040
NUMBER OF PERFORATIONS	7.

RHEOLOGICAL PROPERTIES

SPEED OF COMPRESSION WAVE IN SETTLED BED (IN/SEC)	4000.
SETTLING POROSITY	1.0000
SPEED OF EXPANSION WAVE (IN/SEC)	50000.

SOLID PHASE THERMOCHEMISTRY

MAXIMUM PRESSURE FOR BURN RATE DATA (LBF/IN**2)	100000.
BURNING RATE PRE-EXPONENTIAL FACTOR (IN/SEC/PSI**BN)	.1490E-03
BURNING RATE EXPONENT	.9960
BURNING RATE CONSTANT (IN/SEC)	0.0000
IGNITION TEMPERATURE (DEG.R)	810.0
ARRHENIUS ACTIVATION ENERGY (LBF-IN/LBMOL)	0.
FREQUENCY FACTOR (SEC**-1)	0.
THERMAL CONDUCTIVITY (LBF/SEC/DEG.R)	.2770E-01
THERMAL DIFFUSIVITY (IN**2/SEC)	.1345E-03
EMISSION FACTOR	.000

GAS PHASE THERMOCHEMISTRY

CHEMICAL ENERGY RELEASED IN BURNING (LBF-IN/LBM)	.13100E+08
MOLECULAR WEIGHT (LBM/LBMOL)	21.3300
RATIO OF SPECIFIC HEATS	1.2700
CUVOLUME	30.0000

LOCATION OF PACKAGE(S)

PACKAGE	LEFT BDDY(INS)	RIGHT BDDY(INS)	MASS(LBM)
1	.500	28.480	20.430

PROPERTIES OF PRIMER

CHEMICAL ENERGY RELEASED IN BURNING (LBF-IN/LBM)	.6303E+07
MOLECULAR WEIGHT (LBM/LBMOL)	36.1300
RATIO OF SPECIFIC HEATS	1.2500
SPECIFIC VOLUME OF SOLID (IN**3/LBM)	15.3850

PRIMER DISCHARGE FUNCTION (LBM/IN/SEC)

POS. (INS)	0.00	.49	.50
TIME (SEC)			
0.	12.50	12.50	0.00
.200E-01	12.50	12.50	0.00
.210E-01	0.00	0.00	0.00

PARAMETERS TO SPECIFY TUBE GEOMETRY

DISTANCE (IN)	RADIUS (IN)
0.000	2.730
29.830	2.630
200.000	2.630

WIRE RESISTANCE TABLE

POSITION (INS)	RESISTANCE (PSI)
29.830	100000.
200.000	100000.

THERMAL PROPERTIES OF TUBE

THERMAL CONDUCTIVITY (LBF/SEC/DEG.R)	7.770
THERMAL DIFFUSIVITY (IN**2/SEC)	.2280E-01
EMISSIVITY FACTOR	.700
INITIAL TEMPERATURE (DEG.R)	530.00

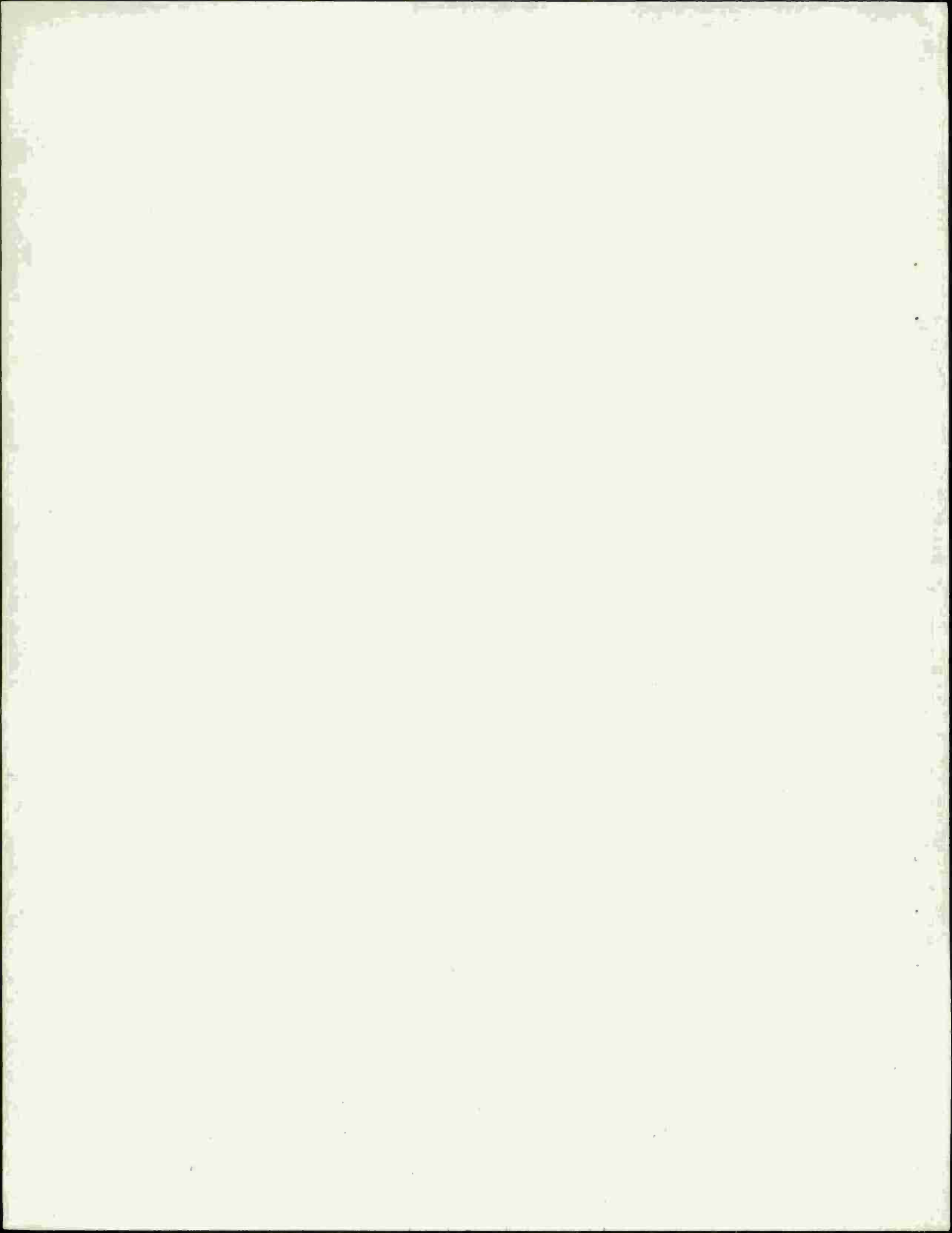
PROJECTILE AND RIFLING DATA

INITIAL POSITION OF BASE OF PROJECTILE (INS)	29.830
MASS OF PROJECTILE (LHM)	103.000
POLAR MOMENT OF INERTIA (LHM-IN**2)	14.000
ANGLE OF RIFLING (DEG)	6.000

POSITIONS FOR PRESSURE TABLE STORAGE

0.0000	4.5000	11.0000	17.5000	24.0000
--------	--------	---------	---------	---------

SETTLING POROSITY AT REFERENCE COMPOSITION HAS BEEN DEFAULTED TO .41233 TO AVOID INITIAL BED COMPACTION OF PROPELLANT TYPE 1



APPENDIX B

NOVA CODE INPUT
1-D CHARGE - M30A1

1-D CHARGE M30A1 (HORSTA)

CONTROL DATA

LOGICAL VARIABLES:

PRINT 1 GRAPH 2 DISK WRITE 0 DISK READ 0
 L.H. TABLE 1 FLAME TABLE 1 PRESSURE TABLE(S) 1
 POSITIVE EFFECT 0 DYNAMIC EFFECT 0 WALL TEMPERATURE CALCULATION 0
 LEFT HAND BOUNDARY CONDITION 0 RIGHT HAND BOUNDARY CONDITION 0 LEFT HAND RESERVOIR 0
 RIGHT HAND RESERVOIR 0 RED PRECOMPRESSED 0
 NOAT LOSS CALCULATION 0 INSULATING LAYER 0

PIPE RESISTANCE FUNCTION 1

INTEGRATION PARAMETERS

NUMBER OF STATIONS AT WHICH DATA ARE STORED 35
 NUMBER OF STEPS BEFORE LOGOUT 100
 TIME STEP FOR DISK START 0
 NUMBER OF STEPS FOR TERMINATION 3500
 TIME FOR TERMINATION (SEC) .2000E-01
 PROJECTILE TRAVEL FOR TERMINATION (INS) 200.00
 MINIMUM TIME STEP (SEC) .1000E-03
 STABILITY SAFETY FACTOR 2.00
 SOURCE STABILITY FACTOR .0500
 SPATIAL RESOLUTION FACTOR .0100
 TIME INTERVAL FOR L.H. TABLE STORAGE (SEC) .1000E-03
 TIME INTERVAL FOR PRESSURE TABLE STORAGE (SEC) .1000E-03

FILE COUNTERS

NUMBER OF STATIONS TO SPECIFY TUBE RADIUS 3
 NUMBER OF TIMES TO SPECIFY PRIMER DISCHARGE 4
 NUMBER OF POSITIONS TO SPECIFY PRIMER DISCHARGE 3
 NUMBER OF ENTRIES IN PIPE RESISTANCE TABLE 2
 NUMBER OF ENTRIES IN WALL TEMPERATURE TABLE 0
 NUMBER OF ENTRIES IN FILLER ELEMENT TABLE 0
 NUMBER OF TYPES OF PROPELLANTS 1
 NUMBER OF BURN RATE DATA SETS 2
 NUMBER OF ENTRIES IN VOID FRACTION TABLE(S) 0 0 0
 NUMBER OF ENTRIES IN PRESSURE HISTORY TABLES 5
 NUMBER OF ENTRIES IN LEFT BOUNDARY SOURCE TABLE 0
 NUMBER OF ENTRIES IN RIGHT BOUNDARY SOURCE TABLE 0
 NUMBER OF WALL STATIONS FOR INVARIANT EMBEDDING 0
 NUMBER OF RED STATIONS FOR INVARIANT EMBEDDING 0
 FRICTION COEFFICIENT 1.0

GENERAL PROPERTIES OF INITIAL AMBIENT GAS

INITIAL TEMPERATURE (DEG.R) 530.0
 INITIAL PRESSURE (PSI) 14.7
 MOLECULAR WEIGHT (G/M/MOLE) 24.000
 RATIO OF SPECIFIC HEATS 1.4000

GENERAL PROPERTIES OF PROPELLANT BED

INITIAL TEMPERATURE (DEG.R) 530.0
 INITIAL MASS CONSTANT (-) 0.000
 VOID FRACTION PACKING COEFFICIENTS 0.0000 0.0000 0.0000

PROPERTIES OF PROPELLANT 1

PROPELLANT TYPE	M30A1
MASS OF PROPELLANT (LBM)	22.2000
DENSITY OF PROPELLANT (LBM/IN**3)	.0585
BURN FUNCTION INDICATOR	7
OUTSIDE DIAMETER (INS)	.4173
INSIDE DIAMETER (INS)	.0338
LENGTH (INS)	.9481
NUMBER OF PERFORATIONS	7.

RHEOLOGICAL PROPERTIES

SPEED OF COMPRESSION WAVE IN SETTLED BED (IN/SEC)	10000.
SETTLING POROSITY	1.0000
SPEED OF EXPANSION WAVE (IN/SEC)	50000.

SOLID PHASE THERMOCHEMISTRY

MAXIMUM PRESSURE FOR BURN RATE DATA (LBF/IN**2)	10000.
BURNING RATE PRE-EXPONENTIAL FACTOR (IN/SEC/PSI**RN)	.6918E-02
BURNING RATE EXPONENT	.5337
MAXIMUM PRESSURE FOR BURN RATE DATA (LBF/IN**2)	60000.
BURNING RATE PRE-EXPONENTIAL FACTOR (IN/SEC/PSI**RN)	.1743E-02
BURNING RATE EXPONENT	.7304
BURNING RATE CONSTANT (IN/SEC)	0.0000
IGNITION TEMPERATURE (DEG.R)	810.0
ARRHENIUS ACTIVATION ENERGY (LBF-IN/LBMOL)	0.
FREQUENCY FACTOR (SEC**-1)	0.
THERMAL CONDUCTIVITY (LBF/SEC/DEG.R)	.2770E-01
THERMAL DIFFUSIVITY (IN**2/SEC)	.1345E-03
EMISSIVITY FACTOR	.500

GAS PHASE THERMOCHEMISTRY

CHEMICAL ENERGY RELEASED IN BURNING (LBF-IN/LBM)	.17600E+04
MOLECULAR WEIGHT (LBM/LBMOL)	23.3000
RATIO OF SPECIFIC HEATS	1.2430
COVOLUME	28.5000

LOCATION OF PACKAGE(S)

PACKAGE	LEFT BODY(INS)	RIGHT BODY(INS)	MASS(LBM)
1	.500	28.350	22.200

PROPERTIES OF PRIMER

CHEMICAL ENERGY RELEASED IN BURNING (LBF-IN/LBM)	.6303E+07
MOLECULAR WEIGHT (LBM/LBMOL)	36.1300
RATIO OF SPECIFIC HEATS	1.2500
SPECIFIC VOLUME OF SOLID (IN**3/LBM)	15.3850

PRIMER DISCHARGE FUNCTION (LBM/IN/SEC)

POS. (INS)	0.00	.25	.26
TIME (SEC)			
0.	5.00	5.00	0.00
.500E-02	25.00	25.00	0.00
.220E-01	25.00	25.00	0.00
.230E-01	0.00	0.00	0.00

PARAMETERS TO SPECIFY TUBE GEOMETRY

DISTANCE (IN)	RADIUS (IN)
0.000	2.730
29.830	2.630
200.000	2.630

ROCK RESISTANCE TABLE

POSITION (INS)	RESISTANCE (PSI)
29.830	100000.
200.000	100000.

THERMAL PROPERTIES OF TUBE

THERMAL CONDUCTIVITY (LBF/SEC/DEG.R)	7.770
THERMAL DIFFUSIVITY (IN**2/SEC)	.2280E-01
EXPANSIVITY FACTOR	.700
INITIAL TEMPERATURE (DEG.R)	530.00

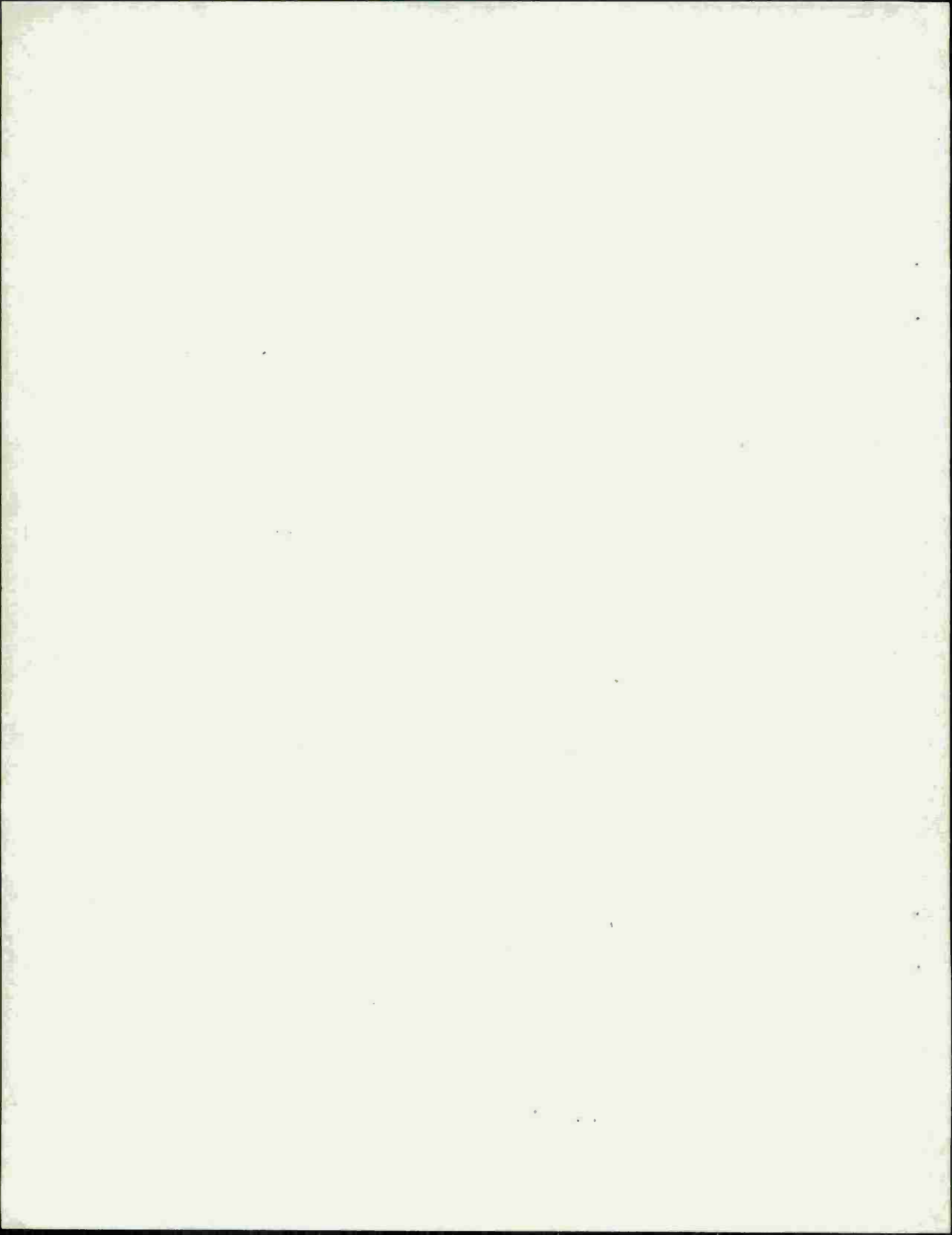
PROJECTILE AND FIFLING DATA

INITIAL POSITION OF BASE OF PROJECTILE (INS)	29.830
MASS OF PROJECTILE (LBM)	103.000
POLAR MOMENT OF INERTIA (LBM-IN**2)	14.000
ANGLE OF TILTING (DEG)	6.000

POSITIONS FOR PRESSURE TABLE STORAGE

0.000	4.5000	11.0000	17.5000	24.0000
-------	--------	---------	---------	---------

SETTLING POROSITY AT REFERENCE COMPOSITION HAS BEEN DEFAULTED TO .39692 TO AVOID INITIAL BED COMPACTION
OF PARTICLE TYPE 1



DISTRIBUTION LIST

<u>No. of</u> <u>Copies</u>	<u>Organization</u>	<u>No. of</u> <u>Copies</u>	<u>Organization</u>
12	Commander Defense Technical Info Center ATTN: DDC-DDA Cameron Station Alexandria, VA 22314	1	Commander US Army Armament Materiel Readiness Command ATTN: DRDAR-LEP-L, Tech Lib Rock Island, IL 61299
1	Director Defense Advanced Research Projects Agency ATTN: E. Blase 1400 Wilson Boulevard Arlington, VA 22209	1	Commander US Army Watervliet Arsenal ATTN: SARWV-RD, R. Thierry Watervliet, NY 12189
1	Director Institute for Defense Analyses ATTN: R. Oliver 400 Army-Navy Drive Arlington, VA 22202	1	Director US Army ARRADCOM Benet Weapons Laboratory ATTN: DRDAR-LCB-TL Watervliet, NY 12189
1	Commander US Army Materiel Development and Readiness Command ATTN: DRCDMD-ST 5001 Eisenhower Avenue Alexandria, VA 22333	1	Commander US Army Aviation Research and Development Command ATTN: DRSAB-E P. O. Box 209 St. Louis, MO 63166
1	Commander US Army Materiel Development and Readiness Command ATTN: DRCDE-DW 5001 Eisenhower Avenue Alexandria, VA 22333	1	Director US Army Air Mobility Research and Development Laboratory Ames Research Center Moffett Field, CA 94035
9	Commander US Army Armament Research and Development Command ATTN: DRDAR-TSS (2 cys) DRDAR-LCA, H. Fair E. Wurzel S. Bernstein D. Downs L. Schlosberg DRDAR-SCA, L. Stiefel DRDAR-LCE, R. Walker Dover, NJ 07801	1	Commander US Army Communications Rsch and Development Command ATTN: DRDCO-PPA-SA Fort Monmouth, NJ 07703
		1	Commander US Army Electronics Research and Development Command Technical Support Activity ATTN: DELSD-L Fort Monmouth, NJ 07703

DISTRIBUTION LIST

<u>No. of Copies</u>	<u>Organization</u>	<u>No. of Copies</u>	<u>Organization</u>
1	Commander US Army Missile Command ATTN: DRSMI-R Redstone Arsenal, AL 35809	1	Director US Army TRADOC Systems Analysis Activity ATTN: ATAA-SL, Tech Lib White Sands Missile Range NM 88002
1	Commander US Army Missile Command ATTN: DRSMI-YDL Redstone Arsenal, AL 35809	1	Chief of Naval Research ATTN: Code 473, R. Miller 800 N. Quincy Street Arlington, VA 22217
1	Commander US Army Missile Command ATTN: DRSMI-RK, R. Rhoades Redstone Arsenal, AL 35809	1	Commander Naval Sea Systems Command ATTN: SEA-62R2, J. Murrin National Center, Bldg. 2 Room 6E08 Washington, DC 20360
1	Commander US Army Natick Research and Development Command ATTN: DRXRE, D. Sieling Natick, MA 01762	5	Commander Naval Surface Weapons Center ATTN: Code G33, J. East D. McClure W. Burrell J. Johndrow Code DX-21, Tech Lib Dahlgren, VA 22448
1	Commander US Army Tank Automotive Research & Development Cmd ATTN: DRDTA-UL Warren, MI 48090	3	Commander Naval Surface Weapons Center ATTN: S. Jacobs, Code 240 Code 730 K. Kim, Code R-13 Silver Spring, MD 20910
2	Commander US Army Materials and Mechanics Research Center ATTN: DRXMR-ATL Tech Lib Watertown, MA 02172	1	Commander Naval Underwater Sys Center Energy Conversion Department ATTN: Code 5B331, R. Lazar Newport, RI 02840
1	Commander US Army Research Office ATTN: Tech Lib P. O. Box 12211 Research Triangle Park NC 27709		

DISTRIBUTION LIST

<u>No. of Copies</u>	<u>Organization</u>	<u>No. of Copies</u>	<u>Organization</u>
2	Commander Naval Weapons Center ATTN: Code 388, R. Derr C. Price China Lake, CA 93555	1	ARO Incorporated ATTN: N. Dougherty Arnold AFS, TN 37389
1	Superintendent Naval Postgraduate School Dept of Mechanical Engineering ATTN: A. Fuhs Monterey, CA 93940	1	Atlantic Research Corp. ATTN: M. King 5390 Cherokee Avenue Alexandria, VA 22314
3	Commander Naval Ordnance Station ATTN: P. Stang S. Mitchell T. Smith Indian Head, MD 20640	1	AVCO Corporation AVCO Everett Rsch Lab Div ATTN: D. Stickler 2385 Revere Beach Parkway Everett, MA 02149
1	AFOSR, Directorate of Aerospace Sciences ATTN: L. Caveny Bolling AFB, DC 20332	1	Calspan Corporation ATTN: E. Fisher P. O. Box 400 Buffalo, NY 14221
2	AFRPL (DYSC) ATTN: D. George J. Levine Edwards AFB, CA 93523	1	Foster Miller Associates, Inc. ATTN: A. Erickson 135 Second Avenue Waltham, MA 02154
1	AFATL (DLDL, O. Heiney) Eglin AFB, FL 32542	1	General Applied Sciences Lab ATTN: J. Erdos Merrick & Stewart Avenues Westbury Long Island, NY 11590
1	Director Lawrence Livermore Laboratory ATTN: M. S. L-355, A. Buckingham P. O. Box 808 Livermore, CA 94550	1	General Electric Company Armament Systems Dept. ATTN: M. Bulman, Rm 1311 Lakeside Avenue Burlington, VT 05402
1	Aerojet Solid Propulsion Co. ATTN: P. Micheli Sacramento, CA 95813	1	Hercules, Inc. Allegany Ballistics Lab ATTN: R. Miller P. O. Box 210 Cumberland, MD 21502

DISTRIBUTION LIST

<u>No. of Copies</u>	<u>Organization</u>	<u>No. of Copies</u>	<u>Organization</u>
1	Hercules, Inc. Bacchus Works ATTN: K. McCarty P. O. Box 98 Magna, UT 84044	1	Pulsepower Systems, Inc. ATTN: L. Elmore 815 American Street San Carlos, CA 94070
1	Hercules, Inc. Eglin Operations AFATL/DL DL (R. Simmons) Eglin AFB, FL 32542	1	Rockwell International Corp. Rocketdyne Division ATTN: BA08, J. Flanagan 6633 Canoga Avenue Canoga Park, CA 91304
1	IITRI ATTN: M. Klein 10 W. 35th Street Chicago, IL 60615	1	Science Applications, Inc. ATTN: R. Edelman 23146 Cumorah Crest Woodland Hills, CA 91364
1	Olin Corporation Badger Army Ammunition Plant ATTN: R. Thiede Baraboo, WI 53913	1	Scientific Research Assoc., Inc. ATTN: H. McDonald P. O. Box 498 Glastonbury, CT 06033
1	Olin Corporation Smokeless Powder Operations ATTN: R. Cook P. O. Box 222 St. Marks, FL 32355	1	Shock Hydrodynamics, Inc. ATTN: W. Anderson 4710-16 Vineland Avenue North Hollywood, CA 91602
1	Paul Gough Associates, Inc. ATTN: P. Gough P. O. Box 1614 Portsmouth, NH 03801	3	Thiokol Corporation Huntsville Division ATTN: D. Flanagan R. Glick Tech Library Huntsville, AL 35807
1	Physics International Co. 2700 Merced Street San Leandro, CA 94577	2	Thiokol Corporation Wasatch Division ATTN: J. Peterson Tech Library P.O. Box 524 Brigham City, UT 84302
1	Princeton Combustion Rsch Laboratory, Inc. ATTN: M. Summerfield 1041 U.S. Highway One North Princeton, NJ 08540	2	United Technology Center ATTN: R. Brown Tech Library P. O. Box 358 Sunnyvale, CA 94088

DISTRIBUTION LIST

<u>No. of</u> <u>Copies</u>	<u>Organization</u>	<u>No. of</u> <u>Copies</u>	<u>Organization</u>
1	Universal Propulsion Company ATTN: H. McSpadden P. O. Box 546 Riverside, CA 92502	1	Institute of Gas Technology ATTN: D. Gidaspow 3424 S. State Street Chicago, IL 60616
1	Battelle Memorial Institute ATTN: Tech Library 505 King Avenue Columbus, OH 43201	1	Johns Hopkins University Applied Physics Laboratory Chemical Propulsion Information Agency ATTN: T. Christian Johns Hopkins Road Laurel, MD 20810
1	Brigham Young University Dept. of Chemical Engineering ATTN: R. Coates Provo, UT 84601	1	Massachusetts Institute of Technology Dept. of Mechanical Engineering ATTN: T. Toong Cambridge, MA 02139
1	California Institute of Tech 204 Karman Lab Mail Stop 301-46 ATTN: F.E.C. Culick 1201 E. California Street Pasadena, CA 91125	1	Pennsylvania State University Applied Research Lab ATTN: G. Faeth P. O. Box 30 State College, PA 16801
1	California Institute of Technology Jet Propulsion Laboratory ATTN: L. Strand 4800 Oak Grove Drive Pasadena, CA 91103	1	Pennsylvania State University Dept. of Mechanical Engineering ATTN: K. Kuo University Park, PA 16801
1	Case Western Reserve University Division of Aerospace Sciences ATTN: J. Tien Cleveland, OH 44135	1	Purdue University School of Mechanical Engineering ATTN: J. Osborn TSPC Chaffee Hall West Lafayette, IN 47906
1	Georgia Institute of Tech School of Aerospace Eng. ATTN: B. Zinn E. Price W. Strahle Atlanta, GA 30332	1	Rutgers State University Dept. of Mechanical and Aerospace Engineering ATTN: S. Temkin University Heights Campus New Brunswick, NJ 08903

DISTRIBUTION LIST

<u>No. of Copies</u>	<u>Organization</u>	<u>No. of Copies</u>	<u>Organization</u>
1	Rensselaer Polytechnic Inst. Department of Mathematics ATTN: D. Drew Troy, NY 12181	1	University of Massachusetts Dept. of Mechanical Engineering ATTN: K. Jakus Amherst, MA 01002
1	SRI International Propulsion Sciences Division ATTN: Tech Library 333 Ravenswood Avenue Menlo Park, CA 94024	1	University of Minnesota Dept. of Mechanical Engineering ATTN: E. Fletcher Minneapolis, MN 55455
1	Stevens Institute of Technology Davidson Laboratory ATTN: R. McAlevy, III Hoboken, NJ 07030	2	University of Utah Dept. of Chemical Engineering ATTN: A. Baer G. Flandro Salt Lake City, UT 84112
1	University of California Los Alamos Scientific Lab ATTN: T3, D. Butler Los Alamos, NM 87554	1	Washington State University Dept. of Mechanical Engineering ATTN: C. Crowe Pullman, WA 99163
1	University of Southern California Mechanical Engineering Dept. ATTN: OHE200, M. Gerstein Los Angeles, CA 90007	<u>Aberdeen Proving Ground</u>	
1	University of California, San Diego AMES Department ATTN: F. Williams P.O. Box 109 La Jolla, CA 92037	Dir, USAMSAA ATTN: DRXSY-D DRXSY-MP, H. Cohen	
1	University of Illinois AAE Department ATTN: H. Krier Transportation Bldg. Rm 105 Urbana, IL 61801	Cdr, USATECOM ATTN: DRSTE-TO-F	
		Dir, USACSL, Bldg. E3516, EA ATTN: DRDAR-CLB-PA	

USER EVALUATION OF REPORT

Please take a few minutes to answer the questions below; tear out this sheet, fold as indicated, staple or tape closed, and place in the mail. Your comments will provide us with information for improving future reports.

1. BRL Report Number _____

2. Does this report satisfy a need? (Comment on purpose, related project, or other area of interest for which report will be used.)

3. How, specifically, is the report being used? (Information source, design data or procedure, management procedure, source of ideas, etc.) _____

4. Has the information in this report led to any quantitative savings as far as man-hours/contract dollars saved, operating costs avoided, efficiencies achieved, etc.? If so, please elaborate.

5. General Comments (Indicate what you think should be changed to make this report and future reports of this type more responsive to your needs, more usable, improve readability, etc.) _____

6. If you would like to be contacted by the personnel who prepared this report to raise specific questions or discuss the topic, please fill in the following information.

Name: _____

Telephone Number: _____

Organization Address: _____

